CDDpress

www.nature.com/cdd

ARTICLE

SCML2 contributes to tumor cell resistance to DNA damage through regulating p53 and CHK1 stability

Qianqian Peng[1,2,5], Xin Shi[1,2,5], Dingwei Li[1,2], Jing Guo[1,2], Xiaqing Zhang[1,2], Xiaoyan Zhang[3,4] and Qiang Chen[1,2]✉

SCML2 has been found to be highly expressed in various tumors. However, the extent to which SCML2 is involved in tumorigenesis and cancer therapy is yet to be fully understood. In this study, we aimed to investigate the relationship between SCML2 and DNA damage response (DDR). Firstly, DNA damage stabilizes SCML2 through CHK1-mediated phosphorylation at Ser570. Functionally, this increased stability of SCML2 enhances resistance to DNA damage agents in p53-positive, p53-mutant, and p53-negative cells. Notably, SCML2 promotes chemoresistance through distinct mechanisms in p53-positive and p53-negative cancer cells. SCML2 binds to the TRAF domain of USP7, and Ser441 is a critical residue for their interaction. In p53-positive cancer cells, SCML2 competes with p53 for USP7 binding and destabilizes p53, which prevents DNA damage-induced p53 overactivation and increases chemoresistance. In p53-mutant or p53-negative cancer cells, SCML2 promotes CHK1 and p21 stability by inhibiting their ubiquitination, thereby enhancing the resistance to DNA damage agents. Interestingly, we found that SCML2A primarily stabilizes CHK1, while SCML2B regulates the stability of p21. Therefore, we have identified SCML2 as a novel regulator of chemotherapy resistance and uncovered a positive feedback loop between SCML2 and CHK1 after DNA damage, which serves to promote the chemoresistance to DNA damage agents.

Cell Death & Differentiation (2023) 30:1849–1867; https://doi.org/10.1038/s41418-023-01184-3

INTRODUCTION

Human Sex comb on midleg like-2 (SCML2), a Polycomb protein containing MBT repeats, has been identified as a component of the noncanonical PRC1 complex in a previous study [1]. The human *SCML2* gene encodes two protein subtypes, SCML2A and SCML2B, which have distinct functions. SCML2B can stabilize p21 and regulate the activation of CDK2/CYCE [2]. Meanwhile, SCML2A binds to PRC1 via its SPM domain and interacts directly with RNA via its RBR domain (RNA-binding region) [1, 3]. Functionally, SCML2A represses PRC1 target genes by targeting chromatin through RNA binding. SCML2 is also involved in facilitating the interaction between PRC1.4 and USP7, through which USP7 regulates the stability of PRC1 components such as BMI1 and RING1B (RNF2) [1]. In mouse, SCML2 only expresses in testes and is essential for male germline [4, 5]. SCML2 participates in mouse spermatogenesis through regulating the epigenetic programming [4, 6–8]. Additionally, high expression of SCML2 has been found in various types of tumors [9–14]. For example, SCML2 has been recognized as a novel marker for gastroenteropancreatic cancers and has been found to promote the progression of hepatocellular carcinoma [10, 12, 13]. Nevertheless, the exact mechanisms linking SCML2 to cancer pathogenesis remain unclear.

The tumor suppressor protein p53 is known to prevent tumorigenesis by triggering cell growth arrest, apoptosis, and senescence [15, 16]. Despite its short lifespan under normal circumstances, p53 quickly becomes stabilized in response to different types of stress to halt the growth and division of damaged and potentially precancerous cells [17–20]. The expression, intracellular translocation, and activity of p53 are precisely regulated by post-translational modifications such as phosphorylation, acetylation, and ubiquitination [20–23]. The ubiquitination process plays a vital role in the degradation of p53 by the proteasome [17, 18]. Mouse double minute 2 homolog (MDM2), an E3 ubiquitin ligase, plays a crucial role in maintaining low levels of p53 as a negative regulator [24, 25]. The ubiquitination of p53 can be reversed by deubiquitinating enzymes (DUBs), including USP7, USP2a, and USP10 [18, 26]. USP7 (HAUSP) is particularly significant as it can regulate the half-life of p53 by directly regulating p53 or its ubiquitin E3 ligase, MDM2. In normal conditions, MDM2 ubiquitinates p53, leading to its low levels, and USP7 binds with MDM2 to prevent it from undergoing autoubiquitination and degradation. Consequently, USP7 decreases p53 levels by stabilizing MDM2 in regular cells [27, 28]. However, after DNA damage, the interaction between MDM2 and p53 is disrupted by phosphorylation. Instead, USP7 directly binds to p53 and stabilizes it by directly removing the ubiquitin molecules from p53 [17, 20, 29]. Given the intricate interplay between USP7, MDM2 and p53, using inhibitors to target USP7 can lead to an increase in p53 levels by disrupting the stability of MDM2, which can ultimately inhibit tumor growth [30, 31]. Other proteins have also

[1]Department of Radiation and Medical Oncology, Medical Research Institute, Zhongnan Hospital of Wuhan University, Wuhan University, Wuhan 430071, PR China. [2]Frontier Science Center for Immunology and Metabolism, Medical Research Institute, Wuhan University, Wuhan, PR China. [3]College of Biomedicine and Health, Huazhong Agricultural University, Wuhan, PR China. [4]College of Life Science and Technology, Huazhong Agricultural University, Wuhan, PR China. [5]These authors contributed equally: Qianqian Peng, Xin Shi. ✉email: Chenq124@whu.edu.cn

Received: 16 October 2022 Revised: 20 May 2023 Accepted: 14 June 2023
Published online: 23 June 2023

been shown to regulate p53 levels by influencing the interactions between USP7 and either MDM2 or p53. For example, RASSF1A promotes the ubiquitination of MDM2, leading to the stabilization of p53 by preventing the interactions between MDM2, DAXX, and USP7 [32]. Meanwhile, TSPYL5 competes with p53 for USP7 binding by physically interacting with USP7, ultimately suppressing p53 activity [33]. EBNA1, on the other hand, reduces p53 stability by competing with p53 for binding with USP7 [34]. Due to the crucial role of p53 in maintaining the integrity of the genome, there is a great deal of interest in identifying novel proteins that regulate the activity of p53, MDM2, and USP7 under various conditions. Identifying such proteins may hold the key to developing more effective drugs for targeting the p53 pathway in disease states such as cancer.

DNA damage agents are commonly employed in medical interventions for treating cancer. However, the use of chemotherapy or radiotherapy often leads to the emergence of cancer cells that are resistant to these agents. Thus, understanding the ways in which cancer cells develop resistance to DNA damage agents is critical for developing effective cancer treatments. After exposure to various stresses, such as DNA damage, the protein p53 is stabilized and activated, leading to the transcription of several target genes involved in different cellular pathways, including cell-cycle arrest, apoptosis, DNA repair, and senescence [16]. Multiple studies have shown that p53 plays a crucial role in determining the sensitivity of cells to DNA damage agents by regulating the cell cycle and DNA damage response (DDR) [35–37]. Moreover, *p21* (*CDKN1A*), a downstream gene of p53, is also involved in determining cell fate following therapy [38–40]. After DNA damage treatment, CHK1 is activated, which controls cell cycle arrest, DNA replication fork stability, and DNA replication origin firing [41]. High expression of CHK1 is commonly observed in various cancer types [42]. Our study shows that SCML2 can influence the resistance of cells to DNA damage agents by modulating p53, p21, and CHK1.

The present study investigated the impact of SCML2 on cell proliferation as well as cancer cell resistance to DNA damage agents. Our findings indicated that SCML2 is upregulated following DNA damage and exhibited distinct effects in p53-positive versus p53-negative or p53-mutant cancer cells, ultimately resulting in increased resistance of cancer cells to DNA damage.

RESULTS

SCML2 depletion decreased cell survival after DNA damage

Initially, we investigated the impact of SCML2 depletion on cell viability after DNA damage. SCML2 depletion in HCT116 cells showed significant decrease of cell survival following treatment with Camptothecin (CPT), Hydroxyurea (HU), Cisplatin or Doxorubicin (Fig. 1A, Supplementary Fig. 1A). The same results were obtained from the investigation performed on A549, Huh7 and NCI-H1299 cells (Fig. 1A, Supplementary Fig. 1A). Notably, HCT116 and A549 cells are p53 wild-type cancer cells, Huh7 is p53 mutant cancer cell and NCI-H1299 cells is p53 negative cancer cell. These results suggested that SCML2 may contribute to the resistance of cancer cells to DNA damage reagents treatment.

To illustrate the role of SCML2 in DNA damage response, we examined whether SCML2 could be affected by DNA damage. The protein level of SCML2 was significantly increased following DNA damage (Fig. 1B), which could be observed by ionizing radiation (IR), CPT, Cisplatin or Doxorubicin treatment. These treatments efficiently led to DNA damage, as shown by the accumulation of γH2AX in cells (Supplementary Fig. 1B). This effect was consistently observed in multiple cancer cell lines (HCT116, A549, Huh7, and NCI-H1299), suggesting that DNA damage-induced increase of SCML2 is a general effect. DNA damage did not affect the mRNA level of SCML2 in p53 wild-type (A549 and HCT116), p53 mutant (Huh7) or p53 negative cells (NCI-H1299) (Fig. 1C, Supplementary Fig. 1C), implying that the stability of SCML2 was upregulated after DNA damage. To confirm the hypothesis that DNA damage stabilizes SCML2, we analyzed the half-life of SCML2 in untreated (UT), CPT, Cisplatin or Doxorubicin treated cells using Cycloheximide (CHX) treatment. The results showed that the half-life of both SCML2A and SCML2B increased after DNA damage (Fig. 1D, Supplementary Fig. 1D). Thus, we uncovered that DNA damage stabilizes SCML2, which may contribute to chemoresistance in cancer cells.

CHK1 stabilized SCML2 after DNA damage through phosphorylation

Protein phosphorylation plays a critical role in DNA damage response (DDR). We overexpressed SFB triple tag (S, Flag and SBP tag) fused SCML2A (SFB-SCML2A) in HEK293T cells. SFB-SCML2A was pull down by S-beads and immunoblotted with anti-Flag and phospho-p-Ser/Thr antibodies. We discovered that SCML2A underwent phosphorylation after CPT treatment, and this modification was prevented by treatment with ATR (AZD6738) or CHK1 inhibitors (AZD7762 or Prexasertib), but not with ATM (KU55933) or DNA-PK (NU7026) inhibitors (Fig. 2A). These findings suggested that the ATR-CHK1 pathway was responsible for CPT-induced SCML2 phosphorylation. Interestingly, the phosphorylation could be detected by both phospho-p-Ser/Thr (p-Ser/Thr) and phospho-SQ/TQ (p-SQ/TQ) antibodies following CPT treatment (Fig. 2A, B). p-SQ/TQ antibody was usually used to detect ATM or ATR substrates after DNA damage, as ATM and ATR share substrate specificity, recognizing Ser-Gln (SQ) and Thr-Gln (TQ) motifs [43, 44]. This phosphorylation could also be observed following Cisplatin or Doxorubicin treatment (Supplementary Fig. 2A). To identify the phosphorylation site, we searched the published database for DNA damage-related SCML2 phosphorylation, and discovered that Ser570, which contains an SQ motif, had been reported to undergo phosphorylation following IR [45]. To confirm whether S570 was the site of DNA damage-induced phosphorylation, the phosphorylation status of a S570A mutant was investigated. The results showed that the DNA damage-induced phosphorylation of SCML2 was significantly reduced in the S570A mutant (Fig. 2C). We constructed a nonrelevant SCML2 S551A mutant as a negative control and found that SCML2 S551A mutant did not affect DNA damage-induced phosphorylation of SCML2 (Supplementary Fig. 2B). These results demonstrated that SCML2 S570 was a major phosphorylation site following DNA damage. To further confirm that Ser570 was a major SCML2 phosphorylation site and that CHK1 directly phosphorylates SCML2 after DNA damage, we conducted an in vitro kinase assay with CHK1 and found that the phosphorylation of the S570A mutant was significantly weaker than the wild-type SCML2 (Fig. 2D). This suggested that SCML2 Ser570 could be phosphorylated by CHK1. Additionally, we confirmed that both SCML2A and SCML2B could be phosphorylated by CHK1 (Supplementary Fig. 2C). Further analysis showed that the DNA damage-induced phosphorylation of SCML2 gradually diminished after release from CPT treatment (Supplementary Fig. 2D), which was consistent with the decrease of CHK1 S345 phosphorylation, a marker for activated CHK1 [46]. These results confirmed that SCML2 was phosphorylated by CHK1 following DNA damage.

We hypothesized that CHK1-mediated S570 phosphorylation may be responsible for the observed increase in SCML2 stability. To test this hypothesis, we treated cells with a CHK1 inhibitor and found that it clearly affected the DNA damage-induced increase in SCML2 protein level (Fig. 2E). Additionally, we created a S570E mutant of SCML2 that mimicked the phosphorylation of S570 and found that this mutant significantly increased the half-life of SCML2 (Fig. 2F). We also used SCML2 S551E as a negative control and found S551E mutant could not increase the stability of SCML2 (Supplementary Fig. 2E). These results strongly suggested that

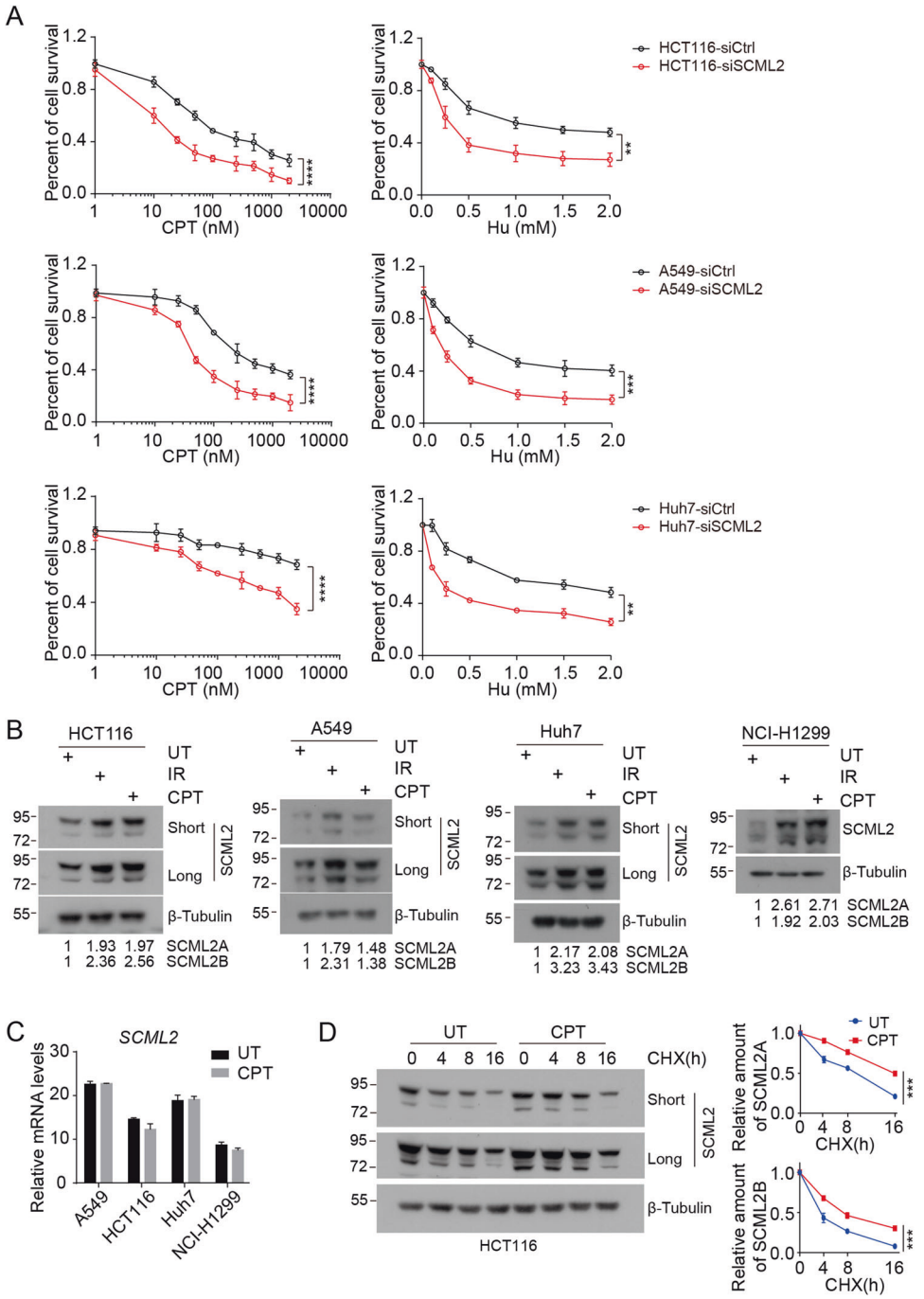

Fig. 1 SCML2 depletion led to decreased cell survival after DNA damage. A CCK8 assay showing cytotoxicity profiles of indicated cell lines as shown. The cells of HCT116, A549 and Huh7 were transfected with the indicated siRNA for 48 h. Then, the cells were treated with camptothecin (CPT, 0, 1, 10, 25, 50, 100, 250, 1000, 2000 nM) for 12 h (Left panel) or hydroxyurea (HU,0, 0.01, 0.025, 0.5, 1, 1.5, 2 mM) for 24 h (Right panel). The cells were changed to fresh medium for an additional 72 h, followed by cell proliferation analysis. The average of three experiments with standard deviations indicated as error bars is shown. $^{**}p < 0.01$, $^{***}p < 0.001$, $^{****}p < 0.0001$. **B** A549, HCT116, Huh7 and NCI-H1299 cells were treated with Ionizing radiation (IR,10 Gy) for 2 h, camptothecin (CPT, 2 μM) for 12 h, or left untreated (UT). The expression of SCML2 proteins was analyzed by western blot. The results of SCML2A and SCML2B were converted into rate measurements and shown on the bottom of each figure. **C** A549, HCT116, Huh7 and NCI-H1299 cells were treated with camptothecin (CPT, 2 μM) for 12 h or untreated (UT). The quantification of SCML2 mRNA was determined by qRT-PCR analysis. **D** Left panel: HCT116 cells were treated with camptothecin (CPT, 2 μM) for 12 h or left untreated (UT), followed by treatment with cycloheximide (CHX, 100 μg/mL) for the indicated times. Cell lysates were then extracted for western blot analysis with the indicated antibodies. Right panel: The SCML2 protein levels were quantified and presented in a plot representing protein half-life. $^{***}p < 0.001$.

CHK1-mediated S570 phosphorylation was responsible for the increase in SCML2 stability after DNA damage.

When treated with the proteasome inhibitor MG132, SCML2 showed an accumulation of ubiquitination and the level of ubiquitination was even stronger in SCML2 S570A (Supplementary Fig. 2F). This suggested that the stability of SCML2 is regulated through proteasome-mediated degradation, and that S570 phosphorylation may protect SCML2 from degradation.

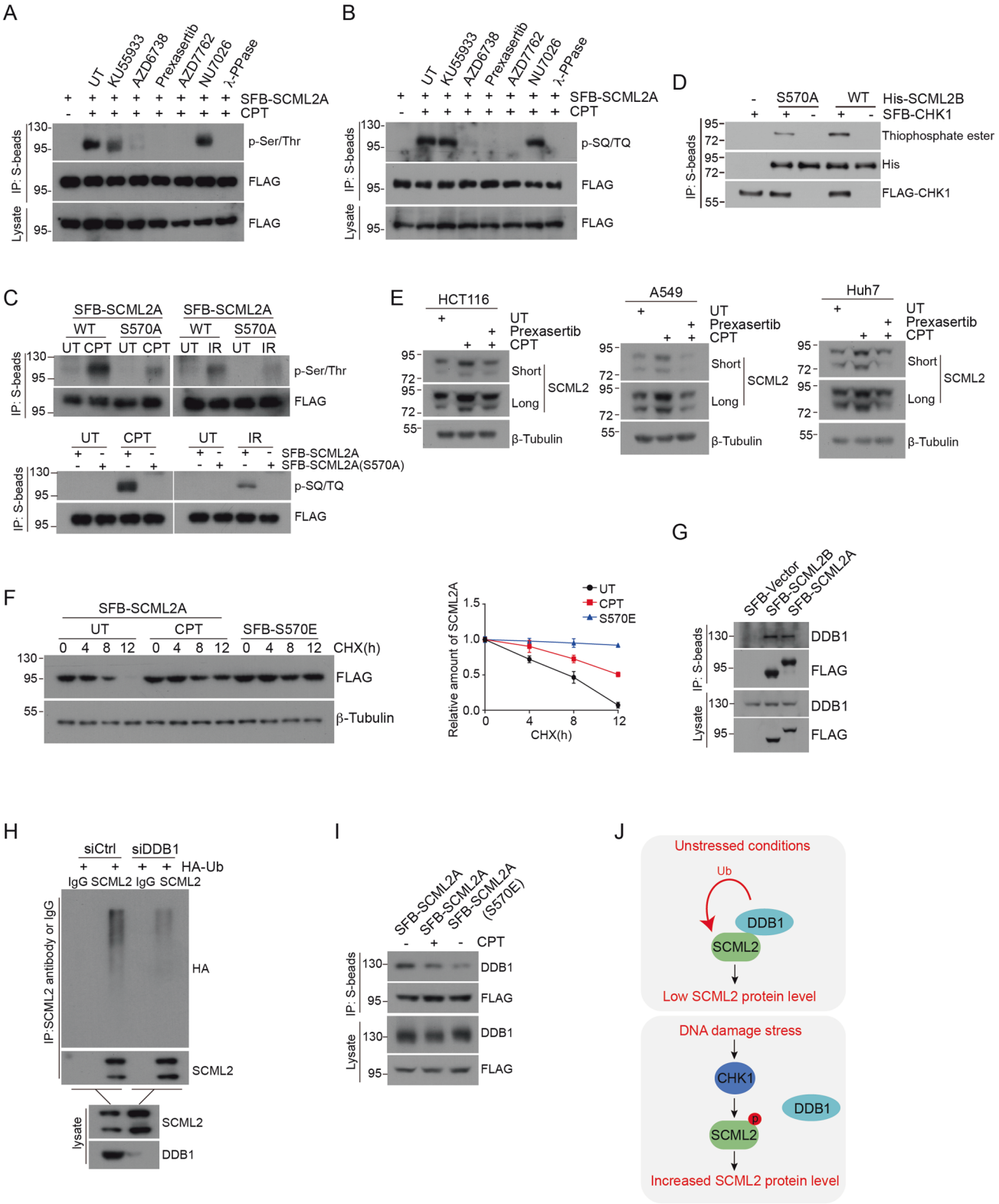

Through unbiased affinity purification, we discovered that DDB1, a component of a ubiquitin E3 complex, is a potential interacting protein of SCML2 (Supplementary Fig. 2G). Further co-immunoprecipitation assays confirmed that both SCML2A and SCML2B interacted with DDB1 (Fig. 2G). Interestingly, depletion of DDB1 was found to decrease SCML2 ubiquitination and stabilize endogenous SCML2 (Fig. 2H), suggesting that DDB1 played a role in regulating SCML2 stability through ubiquitination. Intriguingly, DNA damage or the S570E mutant led to decreased affinity between SCML2 and DDB1 (Fig. 2I, Supplementary Fig. 2H), but not S551E mutant which served as a negative control (Supplementary Fig. 2I), implying that CHK1-mediated S570

Fig. 2 CHK1 stabilized SCML2 after DNA damage through phosphorylation. A, **B** HEK293T cells transfected with SFB-SCML2A plasmid. After 24 h, cells were pretreated with KU55933 (ATM inhibitor, 10 μM), AZD6738 (ATR inhibitor, 1 μM), Prexasertib (CHK1 inhibitor, 250 nM), AZD7762 (CHK1 inhibitor, 60 nM), NU7026 (DNA-PK inhibitor, 10 μM) or untreated (UT) for 1 h, then the cells were untreated (left) or treated with camptothecin (CPT) (2 μM) for an additional 12 h, the expressed SFB-SCML2A was immunoprecipitated with S-beads and immunoblotted with p-Ser/Thr (A) or p-SQ/TQ (B) antibody. **C** HEK293T cells were transfected with SFB-SCML2A (WT) or SFB-SCML2A (S570A). After 24 h, the cells were treated with camptothecin (CPT, 2 μM) for 12 h, Ionizing radiation (IR, 10 Gy) for 2 h or left untreated (UT). Phosphorylation was examined by IP-western analysis using p-SQ/TQ (Upper panel) or p-Ser/Thr antibody (Lower panel). **D** In vitro kinase assay of CHK1. SFB-CHK1 protein was pulled down through S-beads from HEK293T cells. These beads were incubated with purified His-SCML2B-WT or His-SCML2B-S570A proteins as indicated. The phosphorylation of SCML2B was then determined by western blot analysis. **E** HCT116, A549 and Huh7 cells were treated with camptothecin (CPT, 2 μM) alone or both camptothecin (CPT, 2 μM) and Prexasertib (CHK1 inhibitor, 250 nM) for 12 h. The protein level of SCML2 was then determined by western blot. **F** Left panel: HEK293T cells were transfected with SFB-SCML2A (WT) or SFB-SCML2A (S570E) plasmid. After 24 h, the cells with SFB-SCML2A (WT) were treated with camptothecin (CPT, 2 μM) or left untreated (UT) for 12 h, followed by treatment with cycloheximide (CHX, 100 μg/mL) for indicated times. Proteins were extracted and subjected to western blot. Right panel: The protein levels of SCML2A were quantified and a plot representing protein half-life was presented. **G** Determining interactions between SFB-SCML2 and endogenous DDB1 in HEK293T cells by using IP-western. **H** Regulation of SCML2 ubiquitination levels in vivo by DDB1. HEK293T cells were transfected with the indicated siRNAs and HA-Ub. The ubiquitination of SCML2 was immunoprecipitated with anti-SCML2 antibody and immunoblotted with anti-HA and anti-SCML2 antibodies. **I** Interaction of SCML2A with DDB1 in cells. HEK293T cells were transfected with SFB-SCML2A (WT) or SFB-SCML2A (S570E). After 24 h, cells transfected with SFB-SCML2A (WT) were treated with camptothecin (CPT, 2 μM) for 12 h. Cell lysates were immunoprecipitated by S-beads and analyzed by using western blot. **J** Schematic model of SCML2 protein level regulated by DDB1 under unstressed or DNA damage stress conditions. SCML2 binds to DDB1 and is degraded by DDB1-mediated ubiquitination under unstressed condition. However, SCML2 is phosphorylated by CHK1 after DNA damage which prevents the association between DDB1 and SCML2, thus leading to increased SCML2 protein level.

phosphorylation could abrogate DDB1-mediated SCML2 degradation (Fig. 2J). It was worth noting that depletion of USP7 did not have an impact on SCML2 stability, as USP7 depletion did not affect the half-life of SCML2 (Supplementary Fig. 2J).

Thus, we found SCML2 was stabilized after DNA damage through CHK1-mediated S570 phosphorylation.

Ser 441 of SCML2 is the key residue for its association with the TRAF domain of USP7

The level of SCML2 protein was observed to increase in response to DNA damage, suggesting its potential involvement in DDR. Additionally, previous research and our mass spectrum data demonstrated that USP7 is a major binding protein of SCML2 [1] (Supplementary Fig. 2G). USP7 plays a vital role in regulating the stability of p53 after DNA damage [25]. Therefore, SCML2 may participate in DDR via its association with USP7. To explore this possibility, we analyzed the association between SCML2 and USP7.

We confirmed that both SCML2A and SCML2B exhibited almost identical binding capacities with USP7 (Fig. 3A). USP7 is comprised of several domains which interact with different proteins [47], and our findings indicated that the TRAF domain (1-206aa) was responsible for its binding with SCML2 (Fig. 3B). Since the P/AXXS motif is known as a binding motif with the USP7 TRAF domain [48], we analyzed the amino acid sequence of SCML2 and identified five potential binding motifs (Fig. 3C). These motifs were found to be located in various domains of SCML2 (Fig. 3D). Using in vitro GST pull-down and immunoprecipitation assays, we determined that 1-356aa of SCML2 lost its binding capacity with USP7 TRAF domain, while the 25-480aa region retained this ability (Fig. 3E, Supplementary Fig. 3A). This suggested that the binding site was located in the 356-480aa region, which contains two potential binding motifs. After mutating both Pro438 and Ser441 to Ala, SCML2 (25-480aa) lost its ability to bind with USP7 TRAF (Fig. 3F). However, Pro466Ala and Ser469Ala mutant still showed binding ability with USP7 (Fig. 3F), indicating that only PVNS (438-441aa) was the motif responsible for USP7 binding. It is noteworthy that the single mutant Ser441Ala (S441A) significantly hindered its ability to bind with USP7 (Fig. 3F). Moreover, we observed that both SCML2A (S441A) and SCML2B (S441A) lost their ability to bind with USP7 when tested through Co-IP assay in HEK293T cells (Fig. 3G). These findings indicated that Ser441 plays a vital role in the interaction between SCML2 and USP7.

Through MST assay, we compared the binding capacity of SCML2, MDM2, and p53 with USP7 TRAF and revealed that the affinity of SCML2 with USP7 was similar to that of MDM2 and significantly higher than that of p53 (Fig. 3H). In line with the results obtained from the GST-pull down assay, SCML2 (S441A) showed no binding with USP7 in the MST assay (Fig. 3H), demonstrating that SCML2 is a USP7 binding protein and Ser441 is critical for this interaction. The TRAF domain of USP7 plays a crucial role in its binding with p53, and proteins that bind to TRAF can displace p53 and compete with it for USP7 binding [33, 49, 50]. We proposed that SCML2 may also compete with p53 for USP7 binding. To investigate this possibility, we added His-tagged SCML2B or His-tagged SCML2B (S441A) to HEK293T cell lysate and conducted a GST-TRAF pull-down assay (Fig. 3I). The results revealed that as we increased the amount of His-SCML2B, the binding between GST-USP7-TRAF and endogenous p53 gradually reduced, while His-SCML2B (S441A) did not affect this interaction. This suggested that SCML2 can indeed compete with p53 for USP7 binding.

SCML2 prevents p53 overactivation after DNA damage

After DNA damage, the interaction between MDM2 and p53 weakens, resulting in increased p53 stability and activation [17]. Conversely, the association between USP7 and p53 is strengthened following DNA damage [18, 20, 25] (Supplementary Fig. 4A). Therefore, we postulated that SCML2 may compete with p53 for USP7 binding in the presence of DNA damage, thus directly regulating p53 stability. To assess the impact of SCML2A overexpression on p53 stability after DNA damage, we induced the overexpression of SCML2A with varying concentrations of doxycycline (dox) in HCT116 SCML2A Tet-on cells. The results indicated that the levels of both p53 and MDM2 decreased gradually following CPT or Doxorubicin treatment, suggesting that SCML2 may have a negative effect on p53 stability post-DNA damage (Fig. 4A, Supplementary Fig. 4B). Additionally, we examined the mRNA levels of *p53* and its downstream genes after CPT treatment, and found that the *p53* mRNA level remained relatively constant (Fig. 4B). However, overexpression of SCML2A led to a downregulation of p53 downstream genes (Fig. 4B). Meanwhile, SCML2B had a similar function to SCML2A in regulating p53 stability and activation after CPT treatment (Supplementary Fig. 4C, D), although SCML2A exhibited a stronger effect on p53 stability than SCML2B (Supplementary Fig. 4E). We conducted a CHX treatment assay to determine the half-life of p53 following DNA damage and observed that SCML2 overexpression significantly reduced the stability of p53 (Fig. 4C). Furthermore, our findings indicate that SCML2A, but not the SCML2 S441A mutant, can regulate p53 stability and activation following DNA

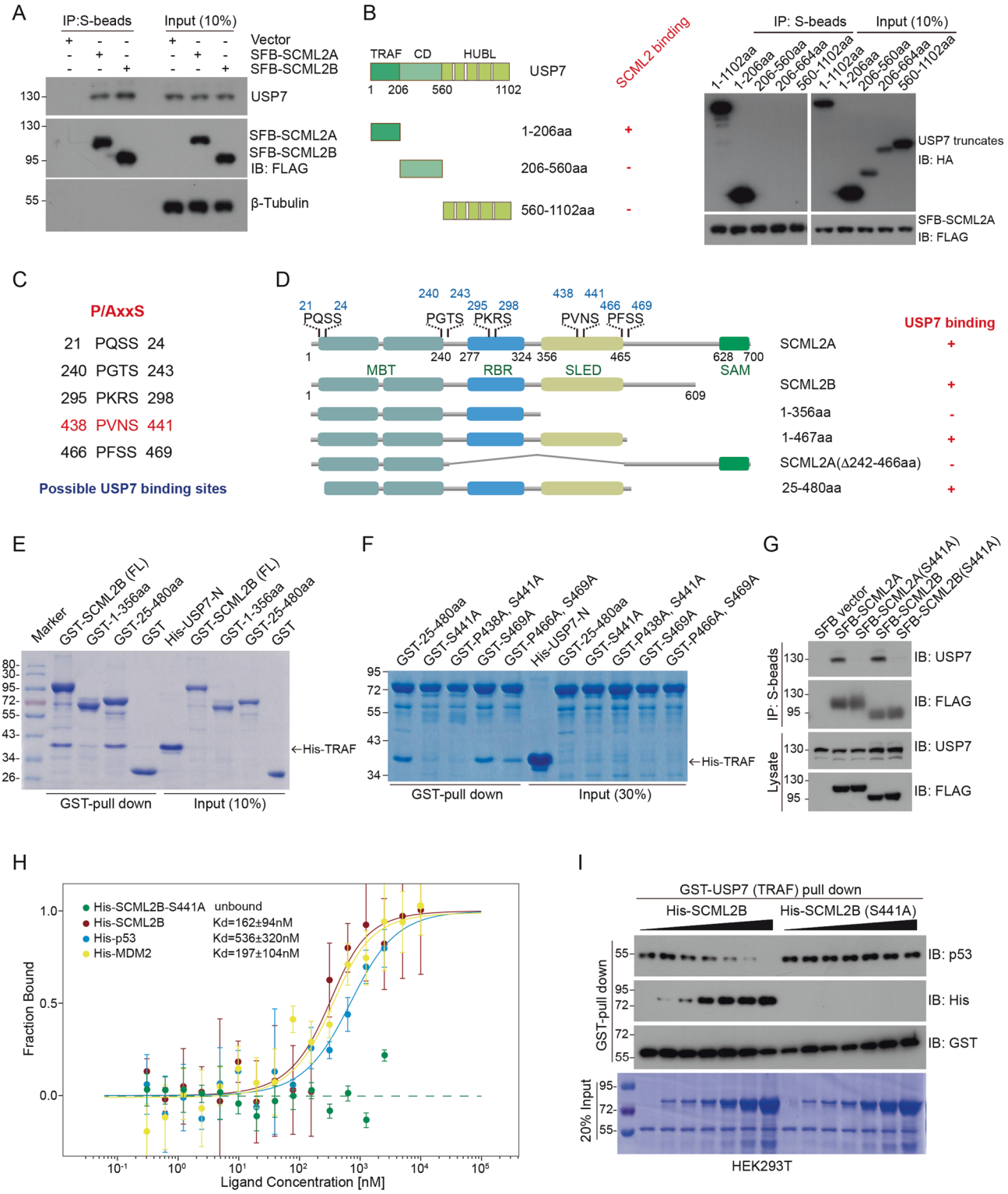

damage (Fig. 4D). This implied that SCML2 may regulate p53 stability and activity through compete with p53 for USP7 binding after DNA damage. To further investigate the impact of SCML2 on p53 after DNA damage, we compared the effects of SCML2 overexpression with treatment with USP7 inhibitor (FT671). The results revealed that SCML2 overexpression had a similar effect to FT671 treatment on the transcription of p53 downstream genes following DNA damage. The combined use of SCML2 overexpression and FT671 treatment resulted in enhanced down-regulation of these genes (Fig. 4E). Moreover, we observed that the protein level of p53 was noticeably higher and its ubiquitination modification was weaker in HCT116 cells depleted of SCML2 compared to wild-type HCT116 cells (Fig. 4F). This suggested that SCML2A may influence p53 stability and activation following DNA damage by impacting USP7-mediated deubiquitylation. These findings indicated that SCML2 competed with p53 for USP7

Fig. 3 Ser 441 of SCML2 is the key residue for its interaction with USP7. A The interaction of SFB-SCML2A, SFB-SCML2B with endogenous USP7 was detected by Co-IP in HEK293T cells. **B** Left panel: A schematic representation of USP7 truncations. Right panel: The interaction of SFB-SCML2A with HA-USP7 truncations was detected by co-immunoprecipitation (Co-IP) in HEK293T cells. Results indicated that the 1-206 amino acid region (TRAF domain) was responsible for mediating this binding. **C** Diagram of predicted SCML2 motifs that may bind to USP7. **D** A schematic representation of SCML2 truncations and their binding ability with USP7, as derived from (**E**), was depicted. **E** GST-pull down assay performed with purified GST-fused full length or truncation constructs of the SCML2B protein and purified His fused USP7-TRAF protein. **F** GST-pull down assay performed with purified GST fused site-directed mutation of the SCML2B protein and purified His fused USP7-TRAF protein. Arrow indicates the positions of His-USP7 TRAF. **G** Co-IP of SCML2 mutation S441A with endogenous USP7 in HEK293T cells. **H** MST analysis of binding of GST-GFP-USP7-TRAF to His-SCML2B-S441A (Green), His-SCML2B (Red), His-p53 (Blue) and His-MDM2 (Yellow). The binding constant, KD, was calculated from the fitted curve for respective ligand protein. All data represent the mean of four independent measurements and error bars represent the standard deviation. **I** GST-pull down experiment verified that SCML2B and p53 compete for direct binding with USP7-TRAF. Purified GST-USP7-TRAF protein was incubated with different amounts (0, 1.25, 2.5, 5, 10, 20, 40 μg) of purified His-SCML2B or SCML2B mutation S441A protein in HEK293T cell lysate, and the captured proteins were detected by western blot.

binding, resulting in the downregulation of p53 stability after DNA damage. We also noted the same effect of SCML2A overexpression on p53 in A549 cells (Fig. 4G). In summary, our results demonstrated that SCML2 had a negative impact on p53 stability and activation following DNA damage.

SCML2 regulates chemoresistance in p53 positive cells

To investigate whether SCML2 regulates cell survival following DNA damage via its binding to USP7, we conducted a CCK8 assay to examine the effect of CPT or HU treatment on cell proliferation. Our results showed that overexpression of either SCML2A or SCML2B significantly increased the resistance of hTERT-RPE1 cells to CPT treatment (as well as HU treatment) compared to control cells (Fig. 5A). The overexpression of SCML2A in RPE1 cells had a significant impact on p53 protein level and its transcriptional activity after DNA damage, in contrast to SCML2A S441A mutant (Supplementary Fig. 5A, B). This suggested that SCML2 may regulate chemoresistance through regulating p53 stability.

To further investigate the influence of SCML2 on the DDR in tumor cells, we generated SCML2 knock-out cells in A549 and HCT116 cell lines, both of which are p53 positive. We also introduced Tet-On inducible SCML2 expression into these knock-out cells (Supplementary Fig. 5C). Our results showed that A549 SCML2 knock-out cells exhibited a significant decrease in cell survival after CPT or HU treatment. Conversely, overexpression of SCML2A or SCML2B in A549 SCML2 knock-out cells restored their resistance to CPT or HU treatment (Fig. 5B). We observed similar results with the HCT116 cell line (Fig. 5C). Furthermore, we analyzed the effect of SCML2 and SCML2 (S441A) overexpression on cell survival following DNA damage. Our results showed that the SCML2A (S441A) and SCML2B (S441A) mutants were unable to fully rescue the defect in cell survival after DNA damage in HCT116 SCML2 knock-out cells (Fig. 5D, E). The same results were observed when HCT16 cells was treated with Cisplatin or Doxorubicin to induce DNA damage (Supplementary Fig. 5D). This suggested that the ability of SCML2 to bind with USP7 contributed to cell resistance to DNA damage (Fig. 5F). Therefore, we identified SCML2 as a novel regulator of chemoresistance in p53 positive cells, by destabilizing p53 and inhibiting its overactivation in response to DNA damage.

As p53 is involved in regulating apoptosis and senescence after DNA damage, we investigated the cellular response to DNA damage under various conditions to determine the fate of the cells. We used Annexin-V apoptosis assay to determine the level of DNA damage-induced cell death. Our results indicated that SCML2 depletion increased cell apoptosis and overexpression of SCML2A or SCML2B (but not SCML2A (S441A) or SCML2B (S441A)) prevented cell apoptosis in HCT116 cells after DNA damage (Supplementary Fig. 5E, F). We used SA-β-gal staining to determine the level of senescence. The results indicated SCML2 depletion or knock-out obviously increased cell senescence after DNA damage (Supplementary Fig. 5G). Overexpression of SCML2A but not SCML2A (S441A) decreased cell senescence in HCT116 SCML2 knock-out cells after DNA damage (Supplementary Fig. 5H). These findings demonstrated that SCML2 regulated DNA damage-induced apoptosis and senescence after DNA damage by competing with p53 for USP7 binding.

SCML2B promotes p21 stability through USP7 binding

Interestingly, we found that SCML2 also promoted cell resistance to DNA damage in Huh7 and H1299 cells, which are p53-mutant or p53-negative cancer cells (Fig. 1A). Therefore, we sought to investigate how SCML2 regulates the chemoresistance of p53 mutant cancer cells. Previous studies have reported that SCML2B can stabilize p21 [2], and elevated levels of p21 protein have been associated with chemoresistance in p53 negative cells [38, 39]. Based on this, we hypothesized that the role of SCML2 in conferring chemoresistance in p53 negative cancer cells may be through the regulation of p21 stability.

We first examined the role of SCML2 in p21 stability. Our analysis showed that depletion of SCML2 led to a decrease in p21 protein levels in HCT116 p53-/- cells (Fig. 6A), indicating that SCML2 regulates p21 through a p53-independent mechanism. As expected, the half-life of p21 was greatly decreased in SCML2 depleted HCT116 p53-/- cells (Fig. 6B) and SCML2 depletion resulted in elevated ubiquitination of p21 (Fig. 6C), indicating that SCML2 may prevent p21 from ubiquitination mediated degradation. The same effect was also observed in p53 positive cancer cells (HCT116 and A549) (Supplementary Fig. 6A). These findings suggested that SCML2 played a role in promoting p21 stability and preventing its degradation through ubiquitination, which did not depend on p53.

To elucidate the role of SCML2 in promoting p21 stability, we investigated the association between SCML2 and p21. Consistent with previous report, we found that SCML2B showed significantly stronger association with p21 than SCML2A when we used GST-p21 to pull down endogenous SCML2 (Fig. 6D). When HEK293T-cells with overexpressing SFB tagged SCML2A or SCML2B was used to conduct GST-pull down assay, we confirmed that SCML2B showed stronger association with p21 than SCML2A (Fig. 6E). Additionally, we found that the N-terminal region of p21 (1-89aa) was responsible for the association between SCML2B and p21 (Fig. 6F). As we observed an increase in SCML2 protein levels after DNA damage, we investigated whether increased SCML2B promoted p21 stability after DNA damage. Treatment with CPT resulted in a significant increase in p21 protein levels in both HCT116 p53-/- and H1299 cells (Fig. 6G). Importantly, SCML2 depletion resulted in a decrease of p21 protein level after CPT treatment (Fig. 6G), indicating that SCML2 played a role in promoting p21 stability after DNA damage.

As SCML2 was a USP7 interacting protein, it is possible that SCML2B linked USP7 with p21 to reduce the ubiquitination of p21. To investigate this possibility, we constructed a Tet-On inducible system to overexpress either wild-type SCML2B or SCML2B (S441A) in H1299 cells. First, we found that overexpression of SCML2B WT, but not the S441A mutant, resulted in an elevation of

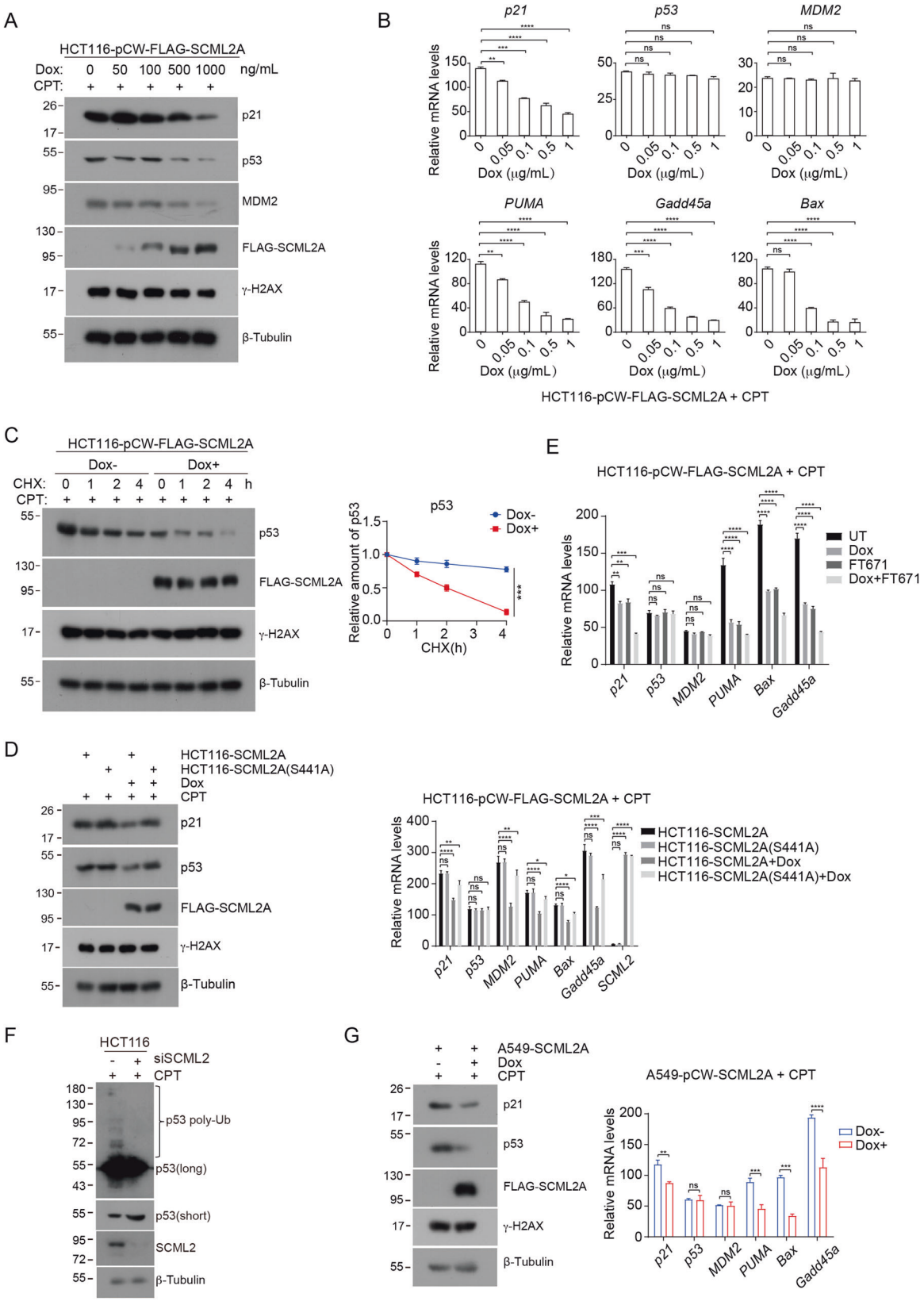

p21 protein levels in both untreated cells and cells treated with CPT (Fig. 6H). Second, we observed that the gradual decrease in p21 levels after release from CPT treatment was delayed in cells overexpressing SCML2B WT (Fig. 6H). These findings indicated that SCML2B may indeed link USP7 to p21 to promote p21 stability. Next, we examined whether the role of SCML2B on p21 stability participated in the regulation of chemoresistance. The cell survival after CPT or HU treatment was analyzed using H1299 SCML2B WT

Fig. 4 SCML2 prevents p53 overactivation after DNA damage. A, **B** HCT116-SCML2A-FLAG Tet-On cell lines pretreated with camptothecin (CPT, 2 μM) for 1 h were treated with doxycycline (Dox) according to the indicated conditions. After 12 h, proteins (A) and mRNA (B) were extracted and subjected to western blot or qRT-PCR. The average of three experiments with standard deviations indicated as error bars is shown. $^{**}p < 0.01$; $^{***}p < 0.001$; $^{****}p < 0.0001$. **C** Following the same pretreatment as described in (**A**, **B**), the cells were subsequently treated with cycloheximide (CHX, 100 μg/mL) and harvested at the indicated times. The levels of p53 protein were analyzed by western blot (Left panel) and a plot representing protein half-life was presented (Right panel: short, short exposure; Long, long exposure). The average of three experiments with standard deviations indicated as error bars is shown. $^{****}p < 0.0001$. **D** HCT116-SCML2A-FLAG and HCT116-SCML2A-S441A-FLAG Tet-On cell lines pretreated with camptothecin (CPT, 2 μM) for 1 h were treated with or without doxycycline (Dox) for 12 h, then proteins (Left panel) and mRNA (Right panel) were extracted and subjected to western blot or qRT-PCR. The average of three experiments with standard deviations indicated as error bars is shown. $^{*}p < 0.05$, $^{**}p < 0.01$, $^{***}p < 0.001$; $^{****}p < 0.0001$. **E** The HCT116-SCML2A-FLAG Tet-On cell lines pretreated with camptothecin (CPT, 2 μM) for 1 h were then treated as follows: untreated (UT); doxycycline (dox, 0.5 μg/mL) for 24 h (Dox); FT671(USP7 inhibitor, 1 μM) for 24 h (FT671); FT671 (1 μM) in combination with doxycycline (Dox, 0.5 μg/mL) for 24 h (Dox+FT671). mRNAs were then extracted and detected to qRT-PCR. The average of three experiments with standard deviations indicated as error bars is shown. $^{**}p < 0.01$, $^{***}p < 0.001$, $^{****}p < 0.0001$. **F** HCT116 cells were transfected with specific siRNA for 72 h. After this, the cells were treated with camptothecin (CPT, 2 μM) for 12 h and then collected. Proteins were extracted and subjected to western blot. **G** The overexpression of SCML2A induced by doxycycline (Dox) leads to different profiles of p53-related genes after DNA damage in A549-SCML2A-FLAG Tet-On cell lines. Proteins and mRNA were extracted and subjected to western blot or qRT-PCR. The average of three experiments with standard deviations indicated as error bars is shown. $^{**}p < 0.01$, $^{***}p < 0.001$, $^{****}p < 0.0001$.

Tet-on cells and H1299 SCML2B (S441A) Tet-on cells. Interestingly, we found that cells overexpressing SCML2B WT exhibited a greater degree of chemoresistance compared to cells overexpressing the S441A mutant (Fig. 6I). Moreover, p21 depletion abolished the chemoresistance induced by SCML2B overexpression (Fig. 6J). These findings suggested that the role of SCML2B on p21 stability contributed to chemoresistance in p53-negative cancer cells.

It has been reported that MDM2 could promote p21 degradation by facilitating binding of p21 with the proteasomal C8 subunit [51]. To exclude the possibility that MDM2 was involved in the regulation of p21 stability by SCML2B, MDM2 was depleted in H1299 SCML2B Tet-on cells. The p21 protein level was examined with or without dox-induced SCML2B overexpression. The results indicated that the effect of MDM2 depletion on the p21 protein level was obviously weaker than the elevation of p21 by SCML2B overexpression in both normal cells and CPT-treated cells (Supplementary Fig. 6B). Meanwhile, MDM2 depletion did not affect SCML2B overexpression-induced p21 stabilization. Thus, these results suggested that MDM2 may be not involved in the regulation of p21 stability by SCML2B.

SCML2 stabilized CHK1 through binding to its CM domain

Given that p21 stability was primarily modulated by SCML2B, we hypothesized that SCML2A may mediate chemoresistance in p53-negative cells via distinct mechanisms. It has been reported that DNA damage leads to the exposure of a degron-like region at the C-terminus of CHK1, which is then targeted for ubiquitination and degradation by the Fbx6-containing Skp1-Cul1-F-box (SCF) E3 ligase [52]. Consistent with previous findings, the level of CHK1 protein significantly decreased in HCT116 p53-/- cells after release from CPT treatment (Fig. 7A). Interestingly, we found that the protein level of CHK1 was greatly reduced in SCML2-depleted HCT116 p53-/- cells following CPT treatment (Fig. 7A), despite no significant changes in mRNA levels (Fig. 7B). Similar results were observed in p53-mutant Huh7 cells after CPT treatment (Fig. 7C). These findings suggest that SCML2 may play a critical role in maintaining CHK1 stability after DNA damage. To confirm these findings, we conducted the same experiment in p53-positive HCT116 cells (Supplementary Fig. 7A) and A549 cells (Supplementary Fig. 7B). In both cases, depletion of SCML2 resulted in decreased CHK1 protein levels following DNA damage, indicating that SCML2 regulates CHK1 protein stability in both p53-positive, p53-mutant, and p53-negative cancer cells. Given that CHK1 plays a crucial role in promoting resistance to DNA damage in cancer cells [42], our findings suggested that SCML2 may enhance chemoresistance by maintaining CHK1 stability.

Interestingly, our results showed that while overexpression of SCML2A (Fig. 7D and Supplementary Fig. 7C) led to a significant elevation in CHK1 protein level after DNA damage in H1299 cells, overexpression of SCML2B had no effect on CHK1 protein level (Fig. 6H, Supplementary Fig. 7D). These findings suggested that CHK1 stability was mainly regulated by SCML2A. To determine if SCML2A promoted chemoresistance in p53 negative cells through regulating CHK1 stability, we examined the chemoresistance of H1299 cells after overexpression of SCML2A. Our results showed that SCML2A overexpression significantly promoted the chemoresistance after treatment with CPT or HU in H1299 cells (Fig. 7E). Furthermore, we found that this chemoresistance was affected by treatment with a CHK1 inhibitor (Prexasertib), suggesting that SCML2A promoted cell survival after DNA damage in p53 negative cancer cells through stabilizing CHK1. It is also interesting to know whether the regulation of CHK1 by SCML2 contributed to SCML2-induced chemoresistance in p53 positive cells. To test this possibility, we conducted the same experiments in HCT116 cells. We found that the chemoresistance induced by SCML2A overexpression was also affected by treatment with a CHK1 inhibitor (Prexasertib) in HCT116 cells (Supplementary Fig. 7E). Remarkably, SCML2 S441A mutant overexpression could also promote chemoresistance in HCT116 cells, which was almost totally abolished by CHK1 inhibitor treatment (Supplementary Fig. 7F), indicating that CHK1 activity was essential for SCML2A S441A induced chemoresistance in p53 wild-type cancer cells. These finding suggested the regulation of CHK1 stability by SCML2 could also contribute to the chemoresistance in both p53 wild-type or p53 negative cancer cells.

Next, we analyzed the underlying mechanism of SCML2 on CHK1 stability. As CHK1 could be degraded by proteasome [52], we investigated SCML2's role in CHK1 ubiquitination. We observed a significant increase in CHK1 ubiquitination in the absence of SCML2 (Fig. 7F). Additionally, following HU treatment, CHK1 ubiquitination was greatly enhanced in SCML2 KO cells compared to HCT116 WT cells (Fig. 7G), implying that SCML2 may prevent CHK1 ubiquitination. Our findings were further substantiated by MG132 treatment, which led to a greater accumulation of ubiquitinated CHK1 in SCML2 KO HCT116 cells than in WT HCT116 cells (Supplementary Fig. 7G). From these results, we concluded that SCML2 played a crucial role in promoting CHK1 stability by inhibiting proteasome-mediated CHK1 degradation. To uncover the mechanism by which SCML2 regulates CHK1 stability, we investigated the interaction between the two proteins. Our results revealed that both SCML2A and SCML2B exhibited binding to the C-terminus of CHK1 (368-476aa, CM domain), rather than the kinase domain (Fig. 7H, Supplementary Fig. 7H). After DNA damage, CHK1 is activated by ATR to establish

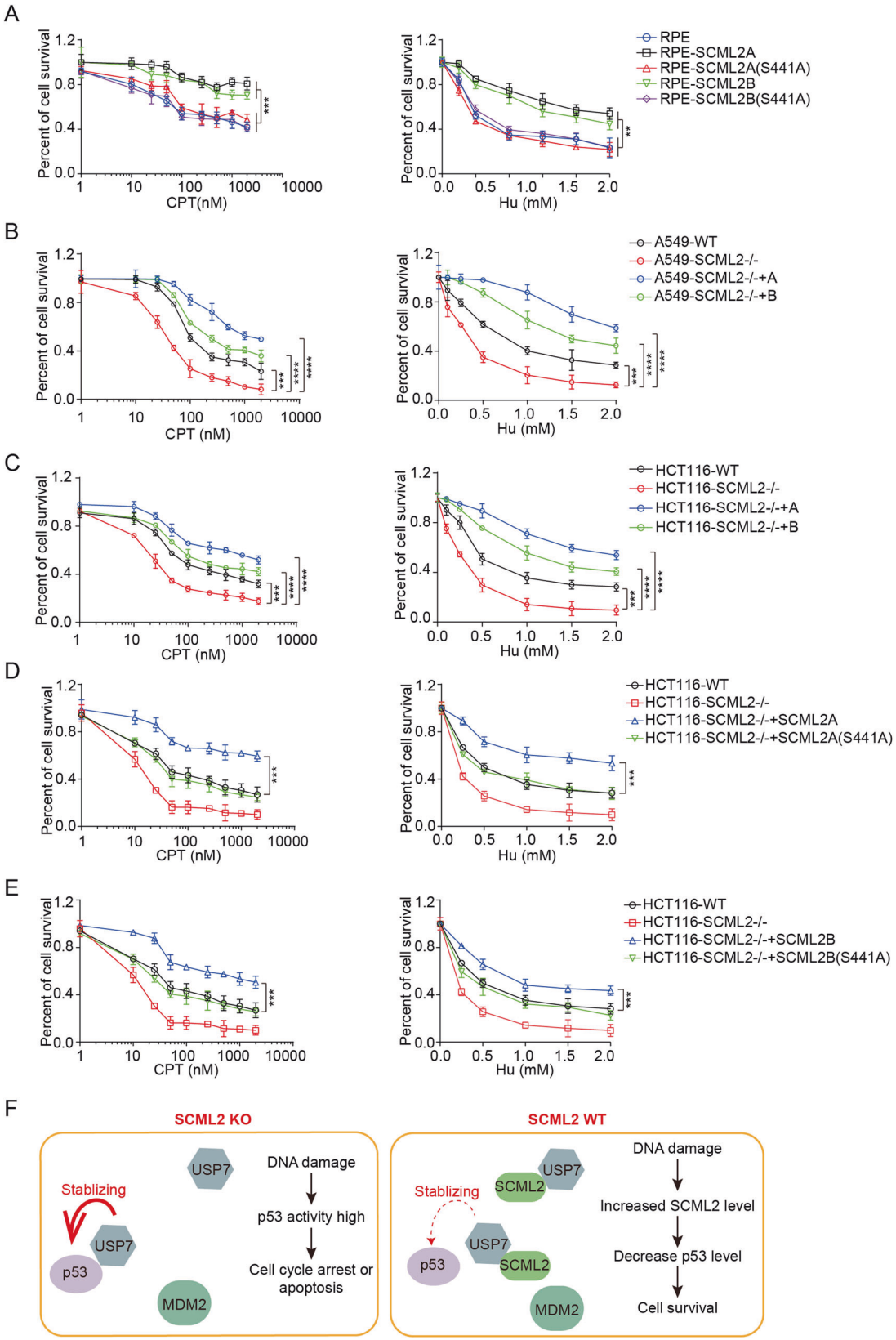

the DNA replication checkpoint and induce G2 arrest [53]. ATR-mediated phosphorylation of CHK1 causes its "closed" conformation to open, blocking the interaction between the kinase domain and C-terminal domain. This ultimately leads to destabilization of CHK1 due to E3 ubiquitin enzymes being able to access the C-terminal region [52, 54]. Since SCML2 binds to the C-terminus (368-476aa) of CHK1, we hypothesized that SCML2 may potentially inhibit the access of E3 to the C-terminus of CHK1, especially after

Fig. 5 SCML2 prevents DNA damage induced cell death in p53 positive cells. A–E CCK8 assay was used to show the cytotoxicity profiles of indicated cell lines. The cells pretreated with 1 μg/mL doxycycline (Dox) for 24 h were treated with camptothecin (CPT, 0, 1, 10, 25, 50, 100, 250, 1000, 2000 nM) for 12 h (Left panel) or hydroxyurea (HU, 0, 0.01, 0.025, 0.5, 1, 1.5, 2 mM) for 24 h (Right panel), then the cells were changed to fresh medium for an additional 72 h, followed by cell proliferation analysis. The average of three experiments, with standard deviations indicated as error bars, was shown. ** $p < 0.01$; ***$p < 0.001$; **** $p < 0.0001$. **A** Comparing the effect of doxycycline (Dox) induced expression of SCML2A, SCML2A(S441A), SCML2B, SCML2B(S441A) with wild-type (WT) RPE1 cells. **B** Four cell lines were used: A549 WT cells, A549 SCML2-/- cells, Tet-On inducible SCML2A expression in A549 SCML2-/- cells, and Tet-On inducible SCML2B expression in A549 SCML2-/- cells. **C** Four cell lines were used: HCT116 WT cells, HCT116 SCML2-/- cells, Tet-On inducible SCML2A expression in HCT116 SCML2-/- cells, and Tet-On inducible SCML2B expression in HCT116 SCML2-/- cells. **D**, **E** The following cells lines were analyzed: HCT116 WT cells, HCT116 SCML2-/- cells, Tet-On inducible SCML2A/B expression in HCT116 SCML2-/- cells, and Tet-On inducible SCML2A/B (S441A) expression in HCT116 SCML2-/- cells. **F** Working model of cell fate determined by SCML2 upon DNA damage. In WT cells, DNA damage leads to increased level of SCML2. These cells with abundant SCML2 expression respond to DNA damage in a positive way by binding to USP7 and compromising p53 activity, which in turn promotes cell survival (Right). SCML2 deletion abolished its ability to jeopardize p53 activity when DNA damage occurred, leading to the tendency of cell cycle arrest and apoptosis (Left).

DNA damage. To confirm this, we first investigated the impact of SCML2 on the ubiquitination of the C-terminus (265-476aa) by inducing SCML2A overexpression with doxycycline. We discovered that SCML2A can effectively prevent the ubiquitination of 265-476aa, and this effect was positively correlated with the expression level of SCML2A (Fig. 7I). Therefore, we identified a novel function of SCML2 in regulating the stability of CHK1 by inhibiting its ubiquitination. Given that both CDT2-Cul4A-DDB1 and SKP1-Cul-Fbx6 have been shown to recognize and ubiquitinate the C-terminus of CHK1 [52, 54], we speculated that SCML2 binding to the same region may hinder the ubiquitination process of these E3 enzymes (Fig. 7J). Therefore, the interaction between CHK1 and SCML2 could establish a positive feedback loop, where CHK1 phosphorylates and stabilizes SCML2 following DNA damage, while the upregulated SCML2, in turn, inhibits the DNA damage-induced ubiquitination of CHK1.

Given the strong correlation between USP7 and SCML2, we investigated whether USP7 also played a role in SCML2-mediated CHK1 stabilization. Firstly, we examined the interaction between CHK1 and USP7 under normal conditions or following treatment with HU (Supplementary Fig. 7I). Consistent with previous report, CHK1 was associated with USP7 [55]. However, while depletion of SCML2 decreased this association under normal conditions, the association between USP7 and CHK1 increased following HU treatment, indicating that this association was independent of SCML2 (Supplementary Fig. 7I). Additionally, overexpression of SCML2A in H1299 cells significantly increased the protein level of CHK1, which was not affected by the USP7 inhibitor FT671 (Supplementary Fig. 7C). These results suggested that SCML2-mediated CHK1 stability following DNA damage was independent of USP7, which differed from the role of SCML2 in the stabilization of p21.

Interestingly, overexpression of SCML2B resulted in a significant increase in p21 protein levels compared to SCML2A overexpression (Supplementary Fig. 7C, D). In contrast, SCML2A overexpression (Fig. 7D) but not SCML2B overexpression (Fig. 6H) significantly increased CHK1 protein levels following DNA damage in H1299 cells. These findings suggested that SCML2A played a more prominent role in regulating CHK1 stability, while SCML2B mainly regulates p21 stability.

SCML2 is upregulated in p53-mutant or p53-negative chemoresistant cancer cells

To investigate whether SCML2 is indeed upregulated to increase the resistance of tumor cells to DNA damage, we utilized CPT treatment to select for a chemoresistant subpopulation from p53-negative H1299 and p53-mutant Huh7 cells. After exposure to 0.5 μM CPT, surviving cells were able to form colonies. We pooled these colonies and repeated the treatment one more time (Fig. 8A). Cells derived from this selection were named H1299-P2 and Huh7-P2 cells, respectively, and these cells exhibited higher levels of SCML2 protein compared to their parental cells (H1299-P0 and Huh7-P0). Notably, the CHK1 and p21 protein levels were also kept at a higher level after CPT treatment in Huh7-P2 (Fig. 8B) and H1299-P2 cells (Fig. 8C), in contrast to their respective parental cells. In addition, we found that knockdown of SCML2 significantly decreased the protein levels of CHK1 and p21 and affected CHK1 activation in these chemoresistant cells (Fig. 8D, E). These results suggested that the elevated levels of SCML2 may contribute to the increased stability of CHK1 and p21 in H1299-P2 and Huh7-P2 cells. Remarkably, both H1299-P2 and Huh7-P2 cells exhibited obvious resistance to HU or CPT treatment compared to H1299-P0 and Huh7-P0 cells. Knockdown of SCML2 or treatment with CHK1 inhibitor in H1299-P2 and Huh7-P2 cells reduced their resistance to HU or CPT treatment (Fig. 8F). These results suggested that the increased protein levels of SCML2 may render the resistance of H1299-P2 and Huh7-P2 to HU or CPT treatment through elevating CHK1 and p21 stability. As both CHK1 and p21 are involved in maintaining G2 arrest after DNA damage [38, 56], it is possible that SCML2 may facilitate the maintenance of G2/M checkpoint and circumvent apoptosis via mitotic catastrophe. In consistent with this hypothesis, we observed that low concentration of MK1775 (50 nM), an inhibitor of WEE1 kinase which plays important roles in maintaining G2/M checkpoint, abolished the resistance to DNA damage induced by SCML2 overexpression in H1299 cells (Fig. 8G). Thus, we concluded that elevated SCML2 protein level following DNA damage facilitated cell survival in p53-negative or p53-mutant cancer cells by enhancing the stability of CHK1 and p21, and maintaining the G2/M checkpoint.

We found that SCML2 promoted the chemoresistance of Huh7 cells, which contains p53 mutant (Y220C). As we have found that SCML2 could stabilize p53 after DNA damage, it is interesting to know whether SCML2 could regulate p53 mutant stability in Huh7 cells. Firstly, we found that p53 mutant in Huh7 cells was aberrantly stable, which was not affected by DNA damage treatment or MDM2 inhibitor treatment (Nutlin-3a) (Supplementary Fig. 8A). Secondly, SCML2 overexpression or SCML2 depletion did not affect the protein level of p53 mutant in Huh7 cells following DNA damage (Supplementary Fig. 8B). Thus, SCML2 could not regulate the stability of p53 mutant in Huh7 cells.

Moreover, the data derived from TCGA database indicated that SCML2 was significantly overexpressed in tumor samples when compared to normal tissues, including colon adenocarcinoma (COAD), liver hepatocellular carcinoma (LIHC), and lung adenocarcinoma (LUAD) (Supplementary Fig. 8C). Remarkably, Kaplan-Meier survival analysis conducted with the GEPIA web server (http://gepia.cancer-pku.cn) on TCGA data revealed that patients with elevated levels of SCML2 expression had a poor overall survival rate than those with low SCML2 expression levels in COAD, LIHC and LUAD (Supplementary Fig. 8D). These findings suggested a significant correlation between SCML2 and tumorigenesis as well as cancer therapy.

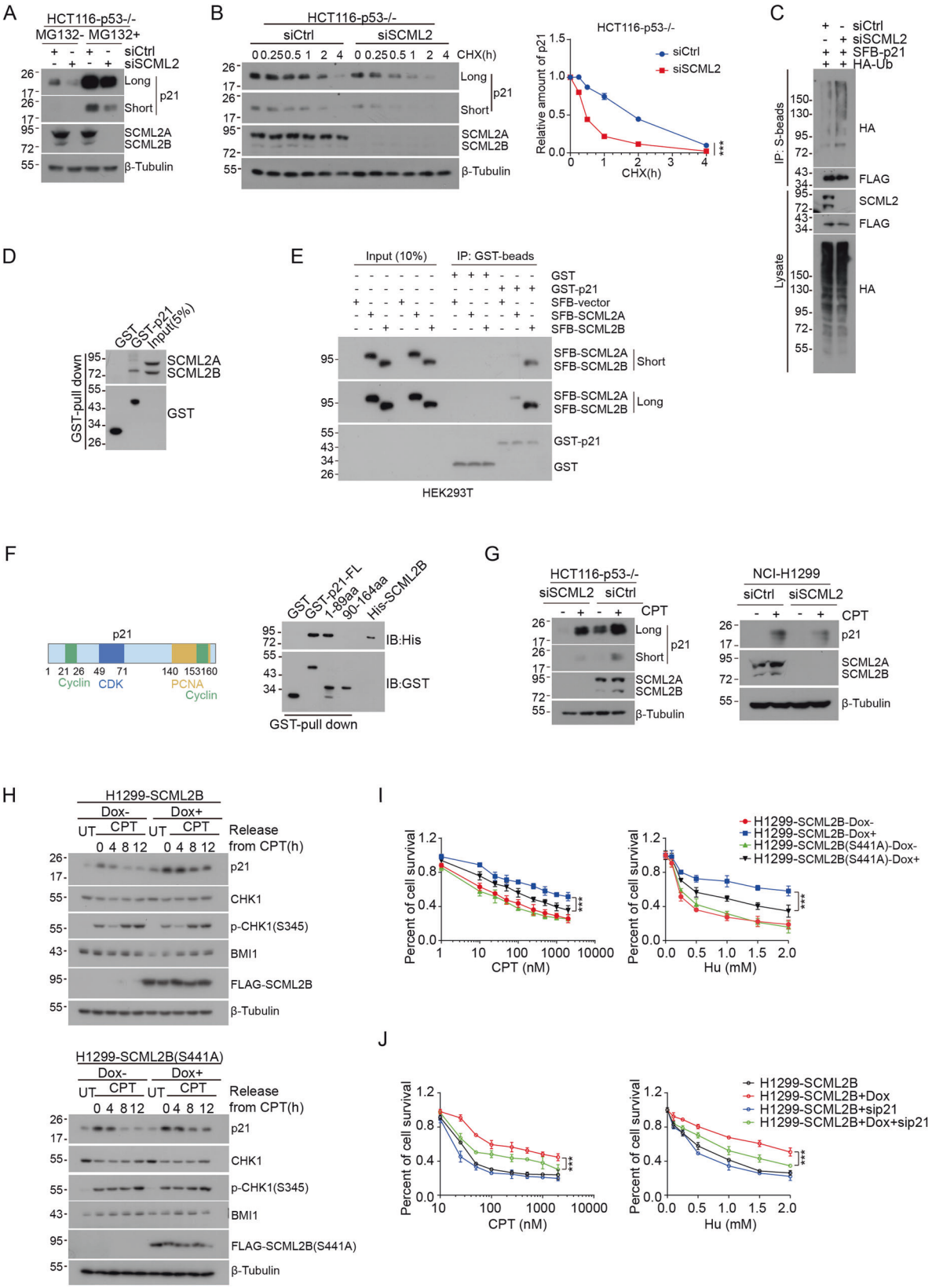

DISCUSSION

Both cancer radiation therapy and chemotherapy aim to eradicate cancer cells by causing direct or indirect DNA damage. However, protein alterations involved in DDR can enable cancer cells to adapt and build resistance to chemotherapy. Tumor suppressor gene *p53*, along with its downstream factor *p21*, plays a crucial role in determining the fate of cancer cells when exposed to radiation or agents that cause DNA damage. Moreover, hyper-activation of CHK1 in cancer cells can also contribute to chemotherapy resistance. In this study, we have identified SCML2

Fig. 6 SCML2 stabilizes p21 through USP7 mediated deubiquitination. A HCT116 p53-/- cells were transfected with siCtrl or siSCML2. After 72 h, the cells were treated with proteasome inhibitor (MG132, 10 μM) or untreated for 6 h. Proteins were extracted and subjected to western blot. **B** HCT116 p53-/- cells were transfected with siCtrl or siSCML2. After 72 h, the cells were treated with cycloheximide (CHX, 100 μg/mL) and harvested at the indicated times. The expression of p21 was determined by western blot (Left panel) and a plot representing protein half-life was presented (Right panel). ***$p < 0.001$. **C** Regulation of p21 ubiquitination levels by SCML2. HEK293T cells pre-transfected with siCtrl or siSCML2 for 60 h were co-transfected with SFB-p21 and HA-Ub. After 24 h, proteins were extracted and subjected to IP-western blot analysis with the indicated antibodies. **D** GST-pull down assay of GST-tagged p21 with endogenous SCML2 in HEK293T cells. **E** The interaction of overexpressing SFB-SCML2A or SFB-SCML2B with purified GST-p21 proteins was detected by GST-pull down in HEK293T cells. **F** Left panel: Schematic representation of p21 truncation constructs. Right panel: In vitro GST-pull down assay using purified GST-fused full length (FL) or truncation constructs of p21 protein and purified His-SCML2B protein. **G** HCT116-p53-/- and NCI-H1299 cells were transfected with siCtrl or siSCML2. After 72 h, the cells were treated with 2 μM camptothecin (CPT) or untreated for 6 h. Proteins were extracted and subjected to western blot. **H** H1299-SCML2B-FLAG and H1299-SCML2B (S441A)-FLAG Tet-On cells pretreated with doxycycline (Dox +) or untreated (Dox-) for 24 h were further treated with 2 μM camptothecin (CPT) for 12 h. These cells were released into fresh medium and harvested at the indicated times. Proteins were extracted and subjected to western blot. **I** Cell viability was determined using CCK8 assay in H1299-SCML2B WT and S441A mutant Tet-On cells. Doxycycline (Dox) induced SCML2B but not SCML2B (S441A) overexpression resulted in reduced sensitivity of H1299 cells to treatment with camptothecin (CPT) (Left) or hydroxyurea (HU) (Right). The average of three experiments, with standard deviations indicated as error bars, was shown. ***$p < 0.001$. **J** The cell viability of Tet-On cells was determined by CCK8 assay. SCML2B overexpression led to reduced sensitivity of cells to treatment with camptothecin (CPT) (Left) or hydroxyurea (HU) (Right). This effect was compromised when p21 was depleted (sip21). The average of three experiments, with standard deviations indicated as error bars, was shown. ***$p < 0.001$.

as a substrate of CHK1 after DNA damage and have further explored the mechanism that links SCML2 stabilization with chemoresistance.

Interplay between SCML2 and CHK1 during DNA damage response

Through our research, we have established that SCML2 undergoes stabilization via CHK1-mediated phosphorylation in cancer cells following DNA damage. Our findings revealed a previously unknown interaction between SCML2 and CHK1 following DNA damage. CHK1 became activated to regulate DNA replication checkpoints, induce G2 cell cycle arrest, and maintain DNA replication fork stability post-DNA damage. We found that SCML2 was a novel substrate of CHK1 following DNA damage, with CHK1 phosphorylating SCML2 at Ser570 to inhibit the association between SCML2 and DDB1. This inhibition subsequently led to an increase in SCML2 stability. Additionally, we discovered that SCML2 could help maintain CHK1 stability via its association with the CM domain (368-476aa) of CHK1. Remarkably, our research highlighted the significant impact of SCML2 on CHK1 stability following DNA damage. ATR phosphorylates CHK1 after DNA damage, which exposes its C terminus for E3 enzyme recognition and subsequent ubiquitination, thereby rendering CHK1 unstable [52, 57]. In this study, we have discovered that SCML2 may prevent this degradation process by inhibiting E3 enzyme recognition of the exposed C terminus of CHK1 after DNA damage. In doing so, SCML2 ultimately facilitated the stabilization of both itself and CHK1. Thus, our findings demonstrated a unique interplay between CHK1 and SCML2 in response to DNA damage.

Notably, Ser570 locates in a SQ motif, which usually recognized by ATM or ATR after DNA damage. Our data has demonstrated that the phosphorylation of SCML2 following DNA damage was reduced in the presence of an ATR inhibitor. While it is possible that ATR directly phosphorylated SCML2, the results of our in vitro phosphorylation assay suggested that CHK1 was capable of directly phosphorylating SCML2, particularly at the Ser570 residue. Moreover, the S570A mutant significantly impacted CHK1-mediated phosphorylation. As CHK1 is mainly activated by ATR following DNA damage, we inferred that the ATR-CHK1 pathway played an important role in DNA damage-induced SCML2 phosphorylation, with CHK1 serving as a direct kinase of SCML2 at the Ser570 residue.

Role of SCML2 in the regulation of chemotherapy resistance

Our findings suggested that SCML2 contributed to the resistance of cancer cells to chemotherapy through two distinct mechanisms (Fig. 8H). First, in p53-positive cells, DNA damage triggers the stabilization and activation of p53, which in turn induces the expression of genes involved in cell cycle arrest, DNA damage repair, apoptosis, and other processes critical for tumor suppression. However, as alterations in the relationship between USP7 and the MDM2-p53 pathway occur following DNA damage [17, 25], SCML2 acted to suppress the stability and activation of p53 by competing with it for binding to USP7. This blockade of p53 activation and stability by SCML2 ultimately led to resistance to DNA-damaging agents. Furthermore, in p53-negative or p53-mutant cancer cells, the absence of p53 activity resulted in defective G1 checkpoint after DNA damage [58–60]. Consequently, these cancer cells are heavily reliant on the CHK1-dependent S and G2/M checkpoints to survive [61, 62]. When SCML2 levels were elevated, CHK1 was notably stabilized, particularly after DNA damage, which triggers the activation of the CHK1-WEE1 pathway to maintain the G2/M checkpoint. By doing so, SCML2 facilitated the promotion and maintenance of G2 cell cycle arrest after DNA damage through CHK1. This extended cell arrest period following DNA damage may allow more time for DNA repair and increase cell survival, leading to chemoresistance in p53-negative cancer cells. In addition, SCML2 played a critical role in promoting the stability of CHK1 in both p53-positive and p53-negative cells, suggesting that the interplay between SCML2 and CHK1 is a general pathway. Additionally, SCML2B facilitated the stability of p21 protein through its association with USP7. It has been reported that elevated levels of p21 protein in p53-negative cancer cells promote their escape from DNA damage-induced senescence and enable them to acquire an aggressive and resistant cancer phenotype in response to chemotherapy [38, 39], This indicated that SCML2B-mediated p21 stabilization also contributed to chemoresistance in p53-negative cancer cells. Thus, SCML2 played a crucial role in regulating the sensitivity or resistance of cancer cells to chemotherapy through distinct mechanisms at play in p53-positive and p53-negative cells.

SCML2A prefers to stabilize CHK1 and SCMLB prefers to stabilize p21

In this study, we have identified distinct mechanisms through which SCML2 regulateed the stability of p53, p21, and CHK1. For p53, both SCML2A and SCML2B competed with p53 for binding to USP7 to control its stability. Interestingly, we found that the effects of SCML2A and SCML2B on CHK1 and p21 were quite different. Consistent with previous reports [2], SCML2B demonstrated a strong interaction with p21, leading to a significant increase in p21 protein levels upon overexpression in H1299 cells, whereas SCML2A overexpression did not have the same effect. Conversely, while both SCML2A and SCML2B showed interaction with CHK1, SCML2A overexpression demonstrated stronger effects on

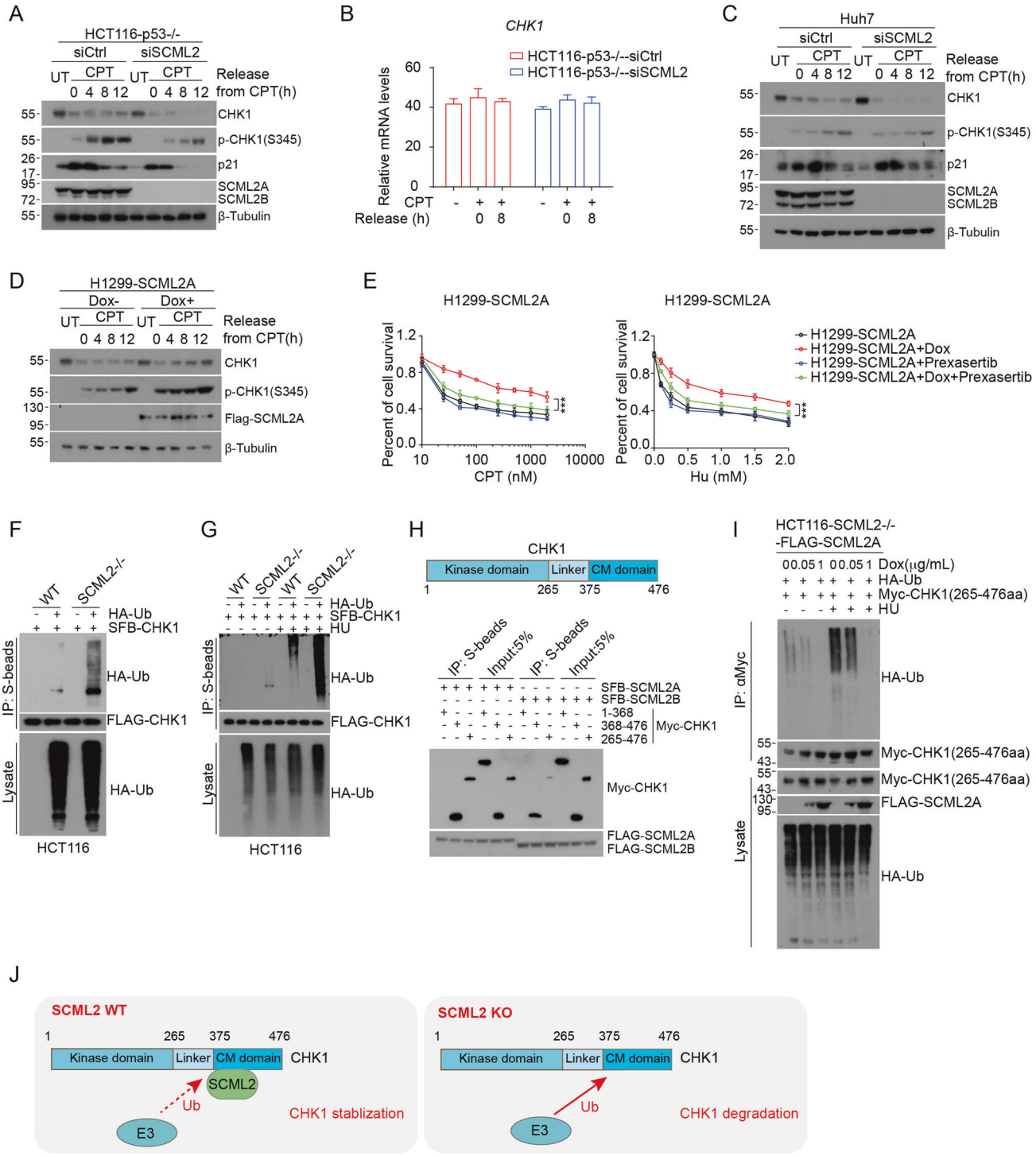

CHK1 stability than SCML2B, which is consistent with the observation that SCML2B exhibited weaker interaction with CHK1 C-terminus than SCML2A (Fig. 7H).

The mechanisms by which SCML2 functioned on p53, p21, and CHK1 were distinct. In the case of p53, SCML2 primarily competed with p53 for USP7 binding after DNA damage. For p21, SCML2B bound to the N-terminus of p21, potentially facilitating the deubiquitinating activity of USP7 on p21. Regarding CHK1, USP7 has been shown to regulate CHK1 stability directly [55] or through ZEB1-mediated interaction [63]. However, USP7 inhibition did not impact the increase of CHK1 induced by SCML2A overexpression, suggesting that USP7 may not contribute to the SCML2A-mediated stabilization of CHK1. Our findings suggested that SCML2 may directly impede the recognition of CHK1 by E3 enzymes FBX6 and DDB1. Notably, as SCML2 has also been found to stabilize BMI1 and RING1B [1], we conducted further experiments to elucidate the specific role of SCML2 on histone modification. Interestingly, we observed that overexpression of SCML2 for a short duration of 24 h did not lead to a significant increase in the protein level of BMI1 (Fig. 6H), indicating that our findings were independent of its effect on histone modification. Thus, our study identified novel functions of SCML2 on p53 and CHK1, which were crucial for chemoresistance.

Fig. 7 SCML2 regulates the stability of CHK1. A HCT116 p53-/- cells were transfected with siCtrl or siSCML2 for 72 h. The cells were then cultured in full medium in the absence (UT) or presence of camptothecin (CPT, 2 μM) for 12 h. The cells were then replaced with fresh medium and harvested at the indicated times. Proteins were extracted and subjected to western blot with indicated antibodies. **B** Cells were treated as Fig. 7A, and mRNAs were extracted and subjected to qRT-PCR. **C** Huh7 cells was analyzed as Fig. 7A. **D** H1299-SCML2A-FLAG Tet-On cells were pre-treated with 1 μg/mL doxycycline (Dox +) or without doxycycline (Dox-) for 24 h. The cells were then treated with camptothecin (CPT, 2 μM) or untreated (UT). After 12 h, the cells were replaced in fresh medium and harvested at the indicated times. Proteins were extracted and subjected to western blot. **E** CCK8 assay showing cytotoxicity profiles of Tet-On cells as shown. The sensitivity of H1299 cells (H1299-SCML2A) or doxycycline-induced SCML2A overexpressing H1299 cells (H1299-SCML2A+Dox) exposed to camptothecin (CPT) (Left) or HU (Right) was analyzed. Treatment with the CHK1 inhibitor (Prexasertib, 50 nM) reduced the resistance to camptothecin (CPT) or hydroxyurea (HU) treatment induced by SCML2A overexpression. The average of three experiments, with standard deviations indicated as error bars, was shown. ***$p < 0.001$. **F** The ubiquitination level of CHK1 was analyzed in HCT116 wild-type (WT) or HCT116 SCML2-/- cells. Indicated cells were transfected with SFB-CHK1 or co-transfected with SFB-CHK1 and HA-Ub for 24 h. Proteins were extracted and immunoprecipitated by S-beads and subsequently analyzed by western blot. **G** The ubiquitination level of CHK1 was analyzed in HCT116 wild-type (WT) or HCT116 SCML2-/- cells after DNA damage. As in (**F**), the transfected cells were treated with or without hydroxyurea (HU, 400 μM) for 24 h. Proteins were extracted and subjected to IP-western blot analysis. **H** Upper panel: A schematic representation of CHK1 truncation constructs. Lower panel: IP-western analysis of HEK293T cells co-transfected with Myc-Chk1 truncations, SFB-SCML2A or SFB-SCML2B for 24 h with indicated antibodies. **I** The analysis was conducted to measure the ubiquitination level of CHK1 (265-476aa) in HCT116-SCML2A-FLAG Tet-On cells under unstressed conditions or after DNA damage. The cells co-transfected with Myc-CHK1 (265-476aa) and HA-Ub for 24 h were treated with doxycycline (Dox) as shown. After 12 h, the cells were treated with hydroxyurea (HU, 400 μM) for 24 h or untreated. Proteins were extracted and subjected to IP-western analysis. **J** Proposed model of CHK1 stability regulated by SCML2. E3 ubiquitin ligases such as DDB1, recognize the C-terminus of CHK1 and induce its ubiquitination for degradation. In WT cells, SCML2 prevents the association between E3 ubiquitin ligases and CHK1, thereby promoting the stability of CHK1. In SCML2-/- cells, E3 ubiquitin ligases facilitates the ubiquitination of CHK1, leading to CHK1 degradation.

Strategies to deal with SCML2 high expression cancer and SCML2 mediated chemoresistance

Our study sheds light on the previously unknown roles of SCML2 in tumor development and unveils its mechanism of action in chemoresistance. Therefore, it is crucial to develop diverse strategies to tackle SCML2-related cancer. In p53-positive tumors, Nutlin 3a, a small molecule inhibitor of MDM2 [64], can be employed to sensitize cancer cells towards chemotherapy by disrupting the SCML2-mediated interplay between USP7 and the MDM2-p53 pathway. Conversely, in p53-negative or p53-mutant cells, where SCML2 facilitates cell cycle arrest through the stabilization of p21 and CHK1 after DNA damage, both CHK1 inhibitors and WEE1 inhibitors could prove effective in overcoming SCML2-mediated chemoresistance.

Limitations of study

Our study has certain limitations that need to be considered. Firstly, SCML2 exists as two isoforms, SCML2A and SCML2B, and their ratios can vary among different cancer cells. However, the mechanisms governing SCML2 splicing are still unclear. Secondly, SCML2 forms a tight association with USP7, and it will be intriguing to investigate if the SCML2/USP7 complex has additional functions. Thirdly, although we examined SCML2's role in different cell lines, our experiments mostly used pooled cells. Further analysis of the molecular dynamics of p53, p21, or CHK1 at the single-cell level using a live-cell reporter system would significantly contribute to elucidating SCML2's precise functions in tumorigenesis and chemoresistance. Finally, as our study was mostly focused on cancer cell lines, it will be crucial to determine whether SCML2 also contributes to chemoresistance of tumors obtained from treated cancer patients.

Finally, our study established the novel role of SCML2 on tumorigenesis and chemoresistance. We also elucidated the mechanism underlying these functions and revealed the new link between SCML2 and p53, p21 and CHK1. These finding may shed new lights on the treatment of tumors with high expression of SCML2.

MATERIALS AND METHODS

Cell culture

Cell lines used in this study were listed in Table S4. All cell lines were maintained in DMEM (Gibco) supplemented with 10% Fetal Bovine Serum (FBS, vol/vol, Gibco) and 1% penicillin-streptomycin (100 U/mL Gibco) and cultured at 37 °C with 5% CO_2.

Generation of knock-out cell lines

All knock-out cell lines (HCT116, A549) used in this study were generated using CRISPR-Cas9 gene editing approach. Briefly, cells were transfected with plasmids that express guide RNAs (gRNAs) against target genes. After 24 h, the cells were selected with puromycin for 36 h and seeded on 96-well plates at low densities (0.5 cells/well), grown for two weeks. Single colonies were picked, and individual clones were validated by sequencing and immunoblot. The guide RNA (gRNA) sequences were listed in Table S2.

Cell line generation

Stable cell lines (RPE1, HCT116, A549, NCI-H1299) were generated using a doxycycline (dox)-inducible Tet-On system (pCW vector). All pCW-related plasmids were constructed by cloning SFB triple tags (S, Flag and SBP tagss) and the target gene into the pCW-cas9 vector. The primers used for the construction of these plasmids can be found in Table S1. Plasmid DNA and lentivirus package plasmids (psPAX2 and pMD2.G) were transfected with polyethylenimine (PEI) into HEK293T cells. After 48 h, the supernatant containing viruses was collected and filtered prior to infection of the indicated cells with polybrene (8 μg/mL) to increase the infection efficiency. After 48 h, puromycin (2 μg/mL) or blasticidin (10 μg/mL) was added to the medium to select for resistant cells. After 10 days, cells were seeded on 96-well plates at low densities (0.5 cells/well) and grown for two weeks. Single cell colonies were picked and expanded. Doxycycline-induced recombinant protein expression levels (0.5-1 μg /mL doxycycline, 12-24 h) were analyzed by western blot using an anti-FLAG antibody. The list of generated cell lines was showed in Table S4.

siRNA transfection and transient transfection

For siRNA targeting assay, cells were transfected with siRNA at a final concentration of 20 nM for the indicated time using Lipofectamine RNAiMAX Reagent (Invitrogen) following the manufacturer's protocol when the cells reached approximate 30–40% confluency. 24 h after transfection, cells were still cultured in fresh medium without penicillin-streptomycin. In general, the interference efficiency was best at 72–96 h after siRNA transfection. The siRNA sequences were indicated in Table S2.

HEK293T cells were transfected using the polyethylenimine (PEI) with DNA/transfection reagent at a 1:3 ratio when the cells reached 70-80% confluency. HCT116 cells were transfected with Lipofectamine 2000 or Lipofectamine 3000 (Thermo Fisher) following the manufacturer's protocol.

Quantative real-time PCR

Total RNA was extracted with TRIzol reagent (15596018; Invitrogen). RNA was reverse transcribed to cDNA by using the PrimeScript RT reagent kit (RR037A; Takara). The synthesized cDNA was used for quantative real-time PCR or RT-PCR assay. Primer sequences were listed in Table S3. Real-time PCR was performed using SYBR Premix Ex Taq (RR420A; TaKaRa) on a CFX96 instrument (Bio-Rad). Sequences of primer pairs used for RT-qPCR in this study, see Table S3.

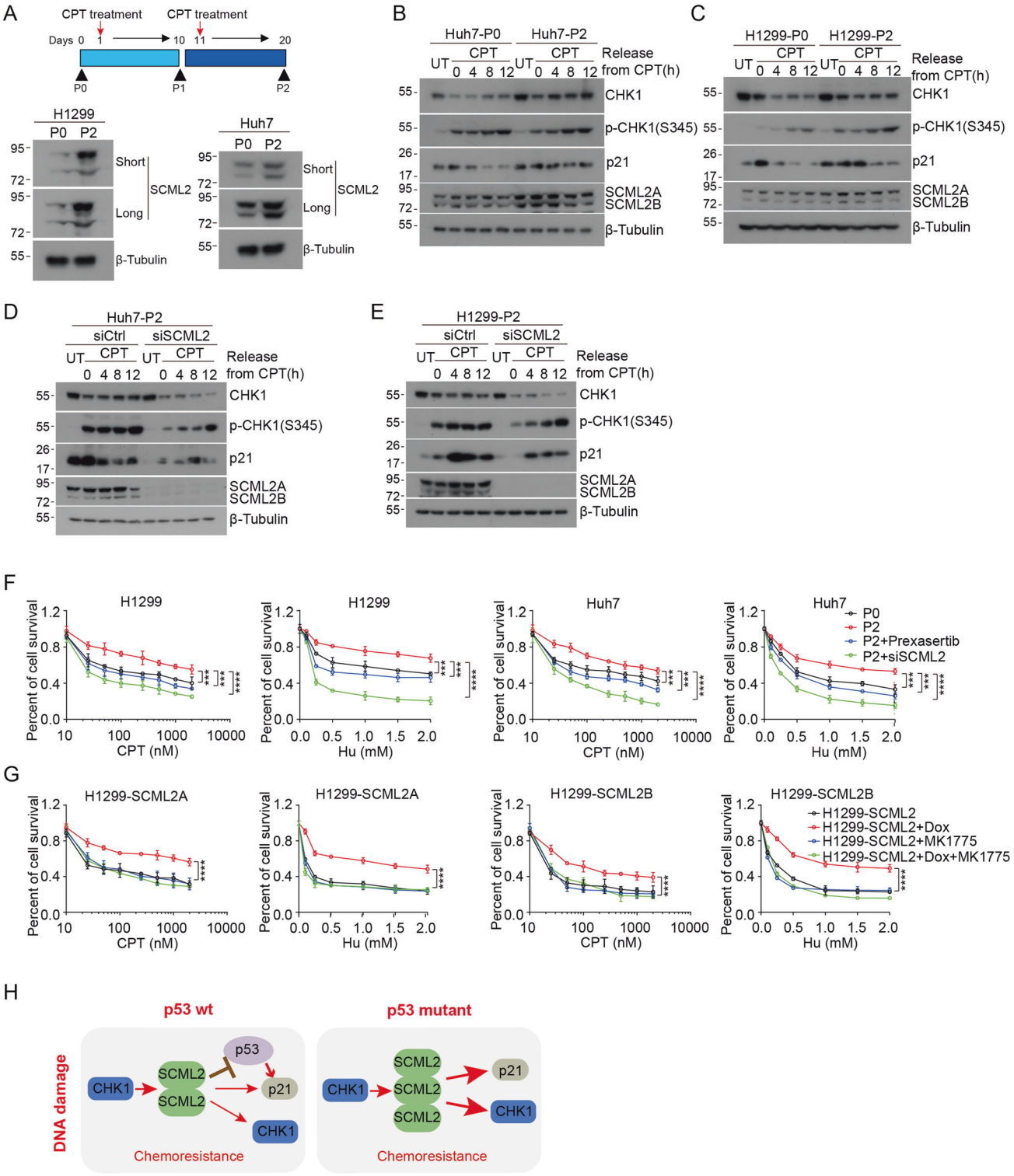

Western blot and Immunoprecipitation

The cells were harvested, washed in PBS, and then lysed in NETN420 buffer (20 mM Tris-HCl pH 8.0, 420 mM NaCl, 0.5% NP-40, 50 mM NaF, 1.5 mM KH_2PO_4, 1 mM EDTA and protease inhibitors) with phosphatase inhibitors on ice for 20 min. The supernatant was then collected by centrifugation (15 min, 12,000 g, 4 °C). Protein concentrations were measured using the BCA protein assay kit (23225; Thermo), and proteins were denatured in 3 x SDS loading buffer with 1 mM DTT (boiled in 95 °C for 10 min). For immunoprecipitation (IP), cell lysates were incubated with 25 µL S agarose beads for IP (3-4 h, 4 °C). For endogenous immunoprecipitation, cell lysates was extracted and then immunoprecipitated with 1 µg of anti-SCML2 antibody or anti-α-IgG rabbit antibody (negative control) (3-4 h, 4 °C), prior to incubation overnight with 30 µL protein G agarose beads. The beads were washed four times in wash buffer (20 mM Tris-HCl pH 8.0, 150 mM NaCl, 0.5% NP-40, 50 mM NaF, 1 mM EDTA and protease inhibitors), and then boiled in 3 x SDS loading buffer with 1 mM DTT (95 °C for 10 min). Input samples (50 µL) were collected before adding antibodies and boiled in 3 x SDS loading buffer with 1 mM DTT (95 °C for 10 min) as well. Total protein in equal amount was then electroblotted onto PVDF membranes (IPVH00010, Merck Millipore). The membranes were blocked in TBST buffer

Fig. 8 SCML2 is upregulated in p53 negative chemoresistant cancer cells. A Experimental strategy for construction of cells used below (Upper panel): P0: untreated cells. P1: P0 cells pretreated with 0.5 μM camptothecin (CPT) for 24 h were cultured for 10 days after changing to fresh medium. P2: P1 cells pretreated with 0.5 μM camptothecin (CPT) for 24 h were cultured for 10 days after changing fresh medium. Lower panel: The expression of SCML2 in the NCI-H1299- P0/P2 (Left) and Huh7-P0/P2 (Right) cell lines. Huh7 (**B**) and H1299 (**C**) cells were treated with camptothecin (CPT, 2 μM) for 12 h and then allowed to recover for the indicated times. Proteins were extracted and subjected to western blot. Huh7-P2 (**D**) and H1299-P2 (**E**) cells were transfected with siCtrl or siSCML2 for 48 h, then treated with camptothecin (CPT, 2 μM) for 12 h. The cells were released into fresh medium and harvested at the indicated times. Proteins were extracted and subjected to western blot. **F** CCK8 assay showing cytotoxicity profiles of cells. Depletion of SCML2 (siSCML2) or CHK1 inhibitor (Prexasertib) treatment increased the sensitivity of H1299-P2 and Huh7-P2 cells to camptothecin (CPT) or hydroxyurea (HU). The average of three experiments, with standard deviations indicated as error bars, was shown. ***$p < 0.001$, **** $p < 0.0001$. **G** CCK8 assay showing cytotoxicity profiles of indicated cells. The sensitivity of H1299-SCML2A and H1299-SCML2B Tet-On cells to camptothecin (CPT) or hydroxyurea (HU) treatment was analyzed. Doxycycline (Dox)-induced expression of SCML2A or SCML2B reduced the sensitivity, which was compromised by Wee1 inhibitor (MK1775, 50 nM) treatment. The average of three experiments, with standard deviations indicated as error bars, was shown. ****$p < 0.0001$. **H** Proposed model for the roles of SCML2 on regulating the chemoresistance in p53 WT or p53 mutant tumor cells after DNA damage.

with 5% non-fat dried milk (RT, 1 h), and washed with TBST, followed by incubation (overnight, 4 °C or RT, 1 h) with primary antibodies and appropriate HRP conjugated secondary antibodies (RT, 1 h) for subsequent detection. The primary antibodies used are listed in key resources table (Table S4). The goat anti-mouse and anti-rabbit secondary antibodies were purchased from Jackson ImmunoReaseach (1414346). Finally, the blots were visualized by using Clarity Western ECL substrate. Antibodies used in this study were listed in Table S4. All the uncropped original western blots used in the manuscript were listed in Original Western blot images file.

Purification of SCML2-associated proteins

Purification of SFB triple-tagged protein (S, FLAG and SBP tags) was described previously [65]. To search for binding proteins of SCML2, we harvested 1 L cultures of 293 T cells stably expressing SFB–SCML2A, and washed the cell pellets with PBS. Cells were lysed with 30 mL ice-cold NETN300 buffer (0.5% NP-40, 50 mM Tris-HCl, pH 8.0, 2 mM EDTA and 300 mM NaCl). The soluble fraction was incubated with 0.5 mL streptavidin-conjugated agarose beads (Millipore, 16-126). The beads were washed with NETN100 buffer (0.5% NP-40, 50 mM Tris-HCl, pH 8.0, 2 mM EDTA and 100 mM NaCl) three times. Associated proteins were eluted with 2 mM biotin (Sigma, B4501) in PBS, and subsequently incubated with 50 μL S-protein Agarose beads (Millipore, 69704). The bound proteins were eluted with SDS sample buffer and analyzed by 10% SDS–PAGE and mass spectrometry. Cells expressing empty vector were used as purification controls.

Cell proliferation assays

Cells at 1000 cells/well/100 μL were seeded in a black wall/clear bottom 96-well plate for 24 h before treatment with indicated reagents for varying time periods as required by the experiment. CCK8 (10 μL/well) was added to the medium, incubated at 37 °C with 5% CO_2 for 2-3 h. The absorbance was measured at 450 nm using a plate reader.

Annexin-V apoptosis assay

To detect apoptosis induced by DNA damage in HCT116 Tet-On cell lines, cells were induced by 0.5 μg/mL doxycycline (dox) after being seeded in 6 cm dishes for 12 h, the cells were treated with camptothecin (CPT, 2 μM) for 12 h, Doxorubicin (10 μM), Hydroxyurea (HU, 400 μM) or Cisplatin (20 μM) for 24 h. Cells were then cultured in fresh medium for 12 h with 0.5 μg/mL doxycycline (dox) at 37 °C with 5% CO_2. Then, 5-10 $\times 10^4$ cells were resuspended in 195 μL annexin-V binding buffer and stained with 5 μL FITC-annexin-V and 10 μL PI, according to the manufacturer's protocol (Beyotime). Finally, flow cytometer was used to analyze stained cells and FITC-PI double positive cells were used to calculate the extent of apoptosis.

SA-β galactosidase assay for senescence

HCT116 and HCT116 Tet-On cells pretreated with 0.5 μg/mL doxycycline for 12 h were treated with camptothecin (CPT, 2 μM) for 12 h, Doxorubicin (10 μM), Hydroxyurea (HU, 400 μM) or Cisplatin (20 μM) for 24 h, and then the cells were cultured for an additional 12 h in fresh medium with 0.5 μg/mL doxycycline (dox). The SA-β galactosidase assay was performed according to the manufacturer's protocol (Beyotime).

Protein purification

All constructs were generated using a standard PCR-based cloning strategy. The GFP-USP7-N fragment was cloned into pGEX-4T-1, while SCML2B-S441A, SCML2B, p53 and MDM2 were cloned into pET-28a. Primers for all the plasmids construction were listed in Table S1. All of the recombinant proteins including GST-GFP-USP7-N, His-SCML2B-S441A, His-SCML2B, His-p53 and His-MDM2 were overexpressed in Escherichia coli strain BL21 cells in medium at 220 rpm in 16 °C overnight. The bacteria were collected by centrifugation at 6000 rpm for 10 min and suspended with His-Tag protein lysis buffer (50 mM Tris-HCl pH 8.0, 0.05% Triton X-100, 250 mM NaCl) or GST-Tag protein lysis buffer (0.5% NP-40, 20 mM Tris-HCl pH 8.0, 100 mM NaCl, 1 mM EDTA pH 8.0) using magnetic stirring. The bacteria were then crushed by high pressure Homogenizer (ATS AH-1500) for 30 min at 4 °C. The supernatant was harvested by centrifugation at 15000 rpm for 30 min, which was added with His-Tag beads or GST-Tag beads and incubated for more than 4 h at 4 °C. Enriched proteins were washed 4 times with His-Tag protein washing buffer (50 mM Tris-HCl pH 8.0, 0.05% Triton X-100, 250 mM NaCl, 20 mM Imidazole) or GST-Tag protein washing buffer (0.5% NP-40, 20 mM Tris-HCl pH 8.0, 100 mM NaCl, 1 mM EDTA) by centrifugation at 8000 rpm for 1 min per time. These beads were eluted by His-Tag protein elution buffer (50 mM Tris-HCl pH 8.0, 0.05% Triton X-100, 250 mM NaCl, 200 mM Imidazole) or GST-Tag protein elution buffer (100 mM Tris-HCl pH 8.0, 1.25% (w/v) Glutathione reduced (Macklin) respectively. Eluents were put into dialysis bags in dialysate (200 mM NaCl, 2.5 mM KCl, 2 mM $Na_2HPO_4{\cdot}12\ H_2O$, 1.5 mM KH_2PO_4) overnight or ultrafiltration device (Millipore) at 4500 rpm for 30 min at 4 °C in order to concentrate proteins.

In vitro protein binding assay by microscale thermophoresis (MST) studies

The ligand proteins including His-SCML2B-S441A, His-SCML2B, His-p53 and His-MDM2 was dissolved in MST buffer (50 mM Tris-HCl pH 7.8, 150 mM NaCl, 10 mM $MgCl_2$) supplemented with 0.05 % Tween 20, and a panel of dilution with 1:1 ratio was prepared using the same buffer, producing ligand concentrations ranging from 610 pM to 20 μM. For the measurement, each diluted ligand was mixed with one volume of target protein GST-GFP-USP7-N, which led to a final concentration of GST-GFP-USP7-N of 300 nM and final ligand concentrations ranging from 305 pM to 10 μM. After 10 min incubation, the samples were loaded into Monolith NT.115 Capillaries (NanoTemper Technologies). MST was measured using a Monolith NT.115 instrument (NanoTemper Technologies) at an ambient temperature of 25 °C. Instrument parameters were adjusted to 50% LED power and medium MST power. Datas of four independently pipetted measurements were analyzed (MO.Affinity Analysis software version 2.3, NanoTemper Technologies) using the signal from an MST on time of 1.5 s.

In vitro binding assay

To produce GST or His fusion proteins, all of the recombinant genes were overexpressed in E. Coli BL21 cells. For the in vitro assay, 2 μg purified recombinant proteins were incubated with 30 μL GST or His-Sepharose beads overnight at 4 °C. For the GST-pull down assay, cells were lysed with NETN420 buffer on ice for 30 min. The supernatant was harvested by centrifugation and incubated with 2 μg GST fusion proteins as well as 30 μL GST-Sepharose beads overnight at 4 °C. The beads were washed 4 times with NENT100 buffer and boiled in 3 x SDS loading buffer with 1 mM DTT (95 °C, 10 min). Finally, the samples were analyzed by western blot.

In vitro kinase assay

For in vitro kinase assay, SFB-Vector or SFB-CHK1 was transfected with PEI into HEK293 cells. After 24 h, the cells were collected and lysed in NETN420 buffer with phosphatase inhibitors on ice for 20 min, followed by

centrifugation at 4 °C and 15,000 g for 10 min to collect supernatant. Subsequently, the cell lysates were incubated with 25 μL S agarose beads in 4 °C for 3 h. After washing with NTEN100, the beads containing 0.1 μg of CHK1 were incubated with 1.2 μg purified His-SCML2B or His-SCML2B (S570A), 1 mM DTT, 0.5 mM ATP-γ-S in 20 μL phosphate kinase buffer (25 mM Tris-HCl at pH7.5, 25 mM KCl, 5 mM $MgCl_2$) for 1 h at 30 °C. The kinase reaction was stopped by adding 0.5 M EDTA. Finally, the mixture was incubated with 50 μM p-Nitrobenzyl mesylate (PNBM) at room temperature for 2 h. The samples were subjected to western blot analysis.

Quantification and statistical analysis

All experiments were performed at least three independent biological replicates in the manuscript. Data was shown as mean ± SD. The significance level was calculated by Student's t-test (two-tailed, equal variance) in GraphPad Prism and P values are shown with $*p < 0.05$, $**p < 0.01$, $***p < 0.001$, $**** p < 0.0001$.

DATA AVAILABILITY

All the uncropped original western blots used in the manuscript were listed in Original Western blot images file in Supplementary materials.

REFERENCES

1. Lecona E, Narendra V, Reinberg D. USP7 cooperates with SCML2 to regulate the activity of PRC1. Mol Cell Biol. 2015;35:1157–68.
2. Lecona E, Rojas LA, Bonasio R, Johnston A, Fernandez-Capetillo O, Reinberg D. Polycomb protein SCML2 regulates the cell cycle by binding and modulating CDK/CYCLIN/p21 complexes. PLoS Biol. 2013;11:e1001737.
3. Bonasio R, Lecona E, Narendra V, Voigt P, Parisi F, Kluger Y, et al. Interactions with RNA direct the Polycomb group protein SCML2 to chromatin where it represses target genes. Elife. 2014;3:e02637.
4. Hasegawa K, Sin HS, Maezawa S, Broering TJ, Kartashov AV, Alavattam KG, et al. SCML2 establishes the male germline epigenome through regulation of histone H2A ubiquitination. Dev Cell. 2015;32:574–88.
5. Luo M, Zhou J, Leu NA, Abreu CM, Wang J, Anguera MC, et al. Polycomb protein SCML2 associates with USP7 and counteracts histone H2A ubiquitination in the XY chromatin during male meiosis. PLoS Genet. 2015;11:e1004954.
6. Adams SR, Maezawa S, Alavattam KG, Abe H, Sakashita A, Shroder M, et al. RNF8 and SCML2 cooperate to regulate ubiquitination and H3K27 acetylation for escape gene activation on the sex chromosomes. PLoS Genet. 2018;14:e1007233.
7. Maezawa S, Hasegawa K, Alavattam KG, Funakoshi M, Sato T, Barski A, et al. SCML2 promotes heterochromatin organization in late spermatogenesis. J Cell Sci. 2018;131:1–12.
8. Maezawa S, Hasegawa K, Yukawa M, Kubo N, Sakashita A, Alavattam KG, et al. Polycomb protein SCML2 facilitates H3K27me3 to establish bivalent domains in the male germline. Proc Nat Acad Sci USA. 2018;115:4957–62.
9. Grubach L, Juhl-Christensen C, Rethmeier A, Olesen LH, Aggerholm A, Hokland P, et al. Gene expression profiling of Polycomb, Hox and Meis genes in patients with acute myeloid leukaemia. Eur J Haematol. 2008;81:112–22.
10. Qi L, Wang L, Huang J, Jiang M, Diao H, Zhou H, et al. Activated amelogenin Y-linked (AMELY) regulation and angiogenesis in human hepatocellular carcinoma by biocomputation. Oncol Lett. 2013;5:1075–9.
11. Shen S, Gui T, Ma C. Identification of molecular biomarkers for pancreatic cancer with mRMR shortest path method. Oncotarget. 2017;8:41432–9.
12. Du L, Wang L, Yang H, Duan J, Lai J, Wu W, et al. Sex comb on midleg like-2 accelerates hepatocellular carcinoma cell proliferation and metastasis by activating Wnt/beta-Catenin/EMT signaling. Yonsei Med J. 2021;62:1073–82.
13. Yang JJ, Huang H, Xiao MB, Jiang F, Ni WK, Ji YF, et al. Sex comb on midleg like-2 is a novel specific marker for the diagnosis of gastroenteropancreatic neuroendocrine tumors. Exp Ther Med. 2017;14:1749–55.
14. Fan T, Jiang G, Shi R, Yu R, Xiao X, Ke D. Construction of AP003469.4-miRNAs-mRNAs ceRNA network to reveal potential biomarkers for hepatocellular carcinoma. Am J Cancer Res. 2022;12:1484–501.
15. Vousden KH, Prives C. Blinded by the Light: The growing complexity of p53. Cell. 2009;137:413–31.
16. Kastenhuber ER, Lowe SW. Putting p53 in context. Cell. 2017;170:1062–78.
17. Shieh SY, Ikeda M, Taya Y, Prives C. DNA damage-induced phosphorylation of p53 alleviates inhibition by MDM2. Cell. 1997;91:325–34.
18. Li M, Chen D, Shiloh A, Luo J, Nikolaev AY, Qin J, et al. Deubiquitination of p53 by HAUSP is an important pathway for p53 stabilization. Nature. 2002;416:648–53.
19. Cummins JM, Rago C, Kohli M, Kinzler KW, Lengauer C, Vogelstein B. Tumour suppression: disruption of HAUSP gene stabilizes p53. Nature. 2004;428:1–2.
20. Meulmeester E, Pereg Y, Shiloh Y, Jochemsen AG. ATM-mediated phosphorylations inhibit Mdmx/Mdm2 stabilization by HAUSP in favor of p53 activation. Cell cycle. 2005;4:1166–70.
21. Lu X, Ma O, Nguyen TA, Jones SN, Oren M, Donehower LA. The Wip1 Phosphatase acts as a gatekeeper in the p53-Mdm2 autoregulatory loop. Cancer Cell. 2007;12:342–54.
22. Rodriguez J, Herrero A, Li S, Rauch N, Quintanilla A, Wynne K, et al. PHD3 regulates p53 protein stability by hydroxylating proline 359. Cell Rep. 2018;24:1316–29.
23. Cui D, Xiong X, Shu J, Dai X, Sun Y, Zhao Y. FBXW7 confers radiation survival by targeting p53 for degradation. Cell Rep. 2020;30:497–509.e494.
24. Moll UM, Petrenko O. The MDM2-p53 interaction. Mol Cancer Res. 2003;1:1001–8.
25. Li M, Brooks CL, Kon N, Gu W. A dynamic role of HAUSP in the p53-Mdm2 pathway. Molecular cell. 2004;13:879–86.
26. Yuan J, Luo K, Zhang L, Cheville JC, Lou Z. USP10 regulates p53 localization and stability by deubiquitinating p53. Cell. 2010;140:384–96.
27. Brooks CL, Gu W. p53 ubiquitination: Mdm2 and beyond. Molecular cell. 2006;21:307–15.
28. Brooks CL, Li M, Hu M, Shi Y, Gu W. The p53-Mdm2-HAUSP complex is involved in p53 stabilization by HAUSP. Oncogene. 2007;26:7262–6.
29. Lee JT, Gu W. The multiple levels of regulation by p53 ubiquitination. Cell Death Differ. 2010;17:86–92.
30. Kategaya L, Di Lello P, Rouge L, Pastor R, Clark KR, Drummond J, et al. USP7 small-molecule inhibitors interfere with ubiquitin binding. Nature. 2017;550:534–8.
31. Wang M, Zhang Y, Wang T, Zhang J, Zhou Z, Sun Y, et al. The USP7 inhibitor P5091 induces cell death in ovarian cancers with different P53 status. Cell Physiol Biochem. 2017;43:1755–66.
32. Song MS, Song SJ, Kim SY, Oh HJ, Lim DS. The tumour suppressor RASSF1A promotes MDM2 self-ubiquitination by disrupting the MDM2-DAXX-HAUSP complex. EMBO J. 2008;27:1863–74.
33. Epping MT, Meijer LA, Krijgsman O, Bos JL, Pandolfi PP, Bernards R. TSPYL5 suppresses p53 levels and function by physical interaction with USP7. Nat Cell Biol. 2011;13:102–8.
34. Saridakis V, Sheng Y, Sarkari F, Holowaty MN, Shire K, Nguyen T, et al. Structure of the p53 binding domain of HAUSP/USP7 bound to Epstein-Barr nuclear antigen 1 implications for EBV-mediated immortalization. Mol Cell. 2005;18:25–36.
35. Tsabar M, Mock CS, Venkatachalam V, Reyes J, Karhohs KW, Oliver TG, et al. A switch in p53 dynamics marks cells that escape from DSB-induced cell cycle arrest. Cell Rep. 2020;32:107995.
36. Porter JR, Fisher BE, Batchelor E. p53 pulses diversify target gene expression dynamics in an mRNA half-life-dependent manner and delineate co-regulated target gene subnetworks. Cell Syst. 2016;2:272–82.
37. Paek AL, Liu JC, Loewer A, Forrester WC, Lahav G. Cell-to-cell variation in p53 dynamics leads to fractional killing. Cell. 2016;165:631–42.
38. Georgakilas AG, Martin OA, Bonner WM. p21: A two-faced genome guardian. Trends Mol Med. 2017;23:310–9.
39. Galanos P, Vougas K, Walter D, Polyzos A, Maya-Mendoza A, Haagensen EJ, et al. Chronic p53-independent p21 expression causes genomic instability by deregulating replication licensing. Nat Cell Biol. 2016;18:777–89.
40. Abbas T, Dutta A. p21 in cancer: intricate networks and multiple activities. Nat Rev Cancer. 2009;9:400–14.
41. Neizer-Ashun F, Bhattacharya R. Reality CHEK: Understanding the biology and clinical potential of CHK1. Cancer Lett. 2021;497:202–11.
42. Zhang Y, Hunter T. Roles of Chk1 in cell biology and cancer therapy. Int J Cancer. 2014;134:1013–23.
43. Kim ST, Lim DS, Canman CE, Kastan MB. Substrate specificities and identification of putative substrates of ATM kinase family members. J Biol Chem. 1999;274:37538–43.
44. O'Neill T, Dwyer AJ, Ziv Y, Chan DW, Lees-Miller SP, Abraham RH, et al. Utilization of oriented peptide libraries to identify substrate motifs selected by ATM. J Biol Chem. 2000;275:22719–27.
45. Matsuoka S, Ballif BA, Smogorzewska A, McDonald ER 3rd, Hurov KE, Luo J, et al. ATM and ATR substrate analysis reveals extensive protein networks responsive to DNA damage. Science. 2007;316:1160–6.
46. Zhao H, Piwnica-Worms H. ATR-mediated checkpoint pathways regulate phosphorylation and activation of human Chk1. Mol Cell Biol. 2001;21:4129–39.
47. Valles GJ, Bezsonova I, Woodgate R, Ashton NW. USP7 is a master regulator of genome stability. Front Cell Dev Biol. 2020;8:717.
48. Sheng Y, Saridakis V, Sarkari F, Duan S, Wu T, Arrowsmith CH, et al. Molecular recognition of p53 and MDM2 by USP7/HAUSP. Nat Struct Mol Biol. 2006;13:285–91.
49. Choi ES, Lee H, Sung JY, Lee CH, Jang H, Kim KT, et al. FAM188B enhances cell survival via interaction with USP7. Cell Death Dis. 2018;9:633.
50. Shen Y, Tu W, Liu Y, Yang X, Dong Q, Yang B, et al. TSPY1 suppresses USP7-mediated p53 function and promotes spermatogonial proliferation. Cell Death Dis. 2018;9:542.

51. Zhang Z, Wang H, Li M, Agrawal S, Chen X, Zhang R. MDM2 is a negative regulator of p21WAF1/CIP1, independent of p53. J Biol Chem. 2004;279:16000–6.
52. Zhang YW, Brognard J, Coughlin C, You Z, Dolled-Filhart M, Aslanian A, et al. The F box protein Fbx6 regulates Chk1 stability and cellular sensitivity to replication stress. Mol Cell. 2009;35:442–53.
53. Saldivar JC, Hamperl S, Bocek MJ, Chung M, Bass TE, Cisneros-Soberanis F, et al. An intrinsic S/G2 checkpoint enforced by ATR. Science. 2018;361:806–10.
54. Leung-Pineda V, Huh J, Piwnica-Worms H. DDB1 targets Chk1 to the Cul4 E3 ligase complex in normal cycling cells and in cells experiencing replication stress. Cancer Res. 2009;69:2630–7.
55. Alonso-de Vega I, Martin Y, Smits VA. USP7 controls Chk1 protein stability by direct deubiquitination. Cell Cycle. 2014;13:3921–6.
56. Liu Q, Guntuku S, Cui XS, Matsuoka S, Cortez D, Tamai K, et al. Chk1 is an essential kinase that is regulated by Atr and required for the G(2)/M DNA damage checkpoint. Genes Dev. 2000;14:1448–59.
57. Huh J, Piwnica-Worms H. CRL4(CDT2) targets CHK1 for PCNA-independent destruction. Mol Cell Biol. 2013;33:213–26.
58. Bieging KT, Mello SS, Attardi LD. Unravelling mechanisms of p53-mediated tumour suppression. Nat Rev Cancer. 2014;14:359–70.
59. Reinhardt HC, Schumacher B. The p53 network: cellular and systemic DNA damage responses in aging and cancer. Trends Genet. 2012;28:128–36.
60. Sherr CJ, McCormick F. The RB and p53 pathways in cancer. Cancer Cell. 2002;2:103–12.
61. Wang Q, Fan S, Eastman A, Worland PJ, Sausville EA, O'Connor PM. UCN-01: a potent abrogator of G2 checkpoint function in cancer cells with disrupted p53. J Natl Cancer Inst. 1996;88:956–65.
62. Ma CX, Janetka JW, Piwnica-Worms H. Death by releasing the breaks: CHK1 inhibitors as cancer therapeutics. Trends Mol Med. 2011;17:88–96.
63. Zhang P, Wei Y, Wang L, Debeb BG, Yuan Y, Zhang J, et al. ATM-mediated stabilization of ZEB1 promotes DNA damage response and radioresistance through CHK1. Nature Cell Biology. 2014;16:864–75.
64. Wang S, Zhao Y, Aguilar A, Bernard D, Yang CY. Targeting the MDM2-p53 protein-protein interaction for new cancer therapy: progress and challenges. Cold Spring Harb Perspect Med. 2017;7:1–10.
65. Chen Q, Chen Y, Bian C, Fujiki R, Yu X. TET2 promotes histone O-GlcNAcylation during gene transcription. Nature. 2013;493:561–4.

AUTHOR CONTRIBUTIONS

QC designed and supervised the study. Q-QP studied the regulation between SCML2 and CHK1. XS constructed all the cell lines and analyzed the regulation between SCML2, USP7 and p21. Q-QP and XS jointly performed the remaining experiments. D-WL performed MST assay. JG and X-QZ generated constructs and purified proteins. QC, XS, X-YZ and Q-QP wrote the manuscript.

FUNDING

QC is supported by grants from the National Key Research and Development Program of China (2018YFC1003400), the National Natural Science Foundation of China (32170698, 31770868) and the Fundamental Research Funds for the Central Universities (2042022dx0003).

COMPETING INTERESTS

The authors declare no competing interests.

ADDITIONAL INFORMATION

Supplementary information The online version contains supplementary material available at https://doi.org/10.1038/s41418-023-01184-3.

Correspondence and requests for materials should be addressed to Qiang Chen.

Reprints and permission information is available at http://www.nature.com/reprints

Publisher's note Springer Nature remains neutral with regard to jurisdictional claims in published maps and institutional affiliations.